Article

Not peer-reviewed version

Extraction and Characterization of Tannins from the Barks of Four Tropical Wood Species and Formulation of Bio-Resins for Potential Industrial Applications

Liliane Nga , Benoit Ndiwe * , Achille Bernard Biwole , Jean Jalin Eyinga Biwole , Mewoli Armel , Joseph Zobo Mfomo , Anélie Petrissans , Antonio Pizzi , Antonios N Papadopoulos *

Posted Date: 10 June 2025

doi: 10.20944/preprints202506.0750.v1

Keywords: tannins; tropical wood barks; bio-based resins; characteristics; applications

Article

Extraction and Characterization of Tannins from the Barks of Four Tropical Wood Species and Formulation of Bio-Resins for Potential Industrial Applications

Liliane Nga [1], Benoit Ndiwe [1,2,*], Achille Bernard Biwole [1], Jean Jalin Eyinga Biwole [1], Mewoli Armel [3], Joseph Zobo Mfomo [1], Anélie Petrissans [4], Antonio Pizzi [4] and Antonios N. Papadopoulos [5,*]

[1] Laboratory of Forest Resources and Wood Valorization, Training Unit in Engineering Sciences, Post Graduate School of Fundamental and Applied Sciences, University of Douala, P.O. Box 1872, Douala, Cameroun

[2] Laboratory of Mechanics, Training Unit in Engineering Sciences, Post Graduate School of Fundamental and Applied Sciences, University of Douala, P.O. Box 2701, Douala, Cameroun

[3] Department of Industrial and Mechanical Engineering, University of Yaoundé 1, National Advanced School of Engineering, P.O. Box. 8390, Yaoundé, Cameroon

[4] Laboratory of Studies and Research on Wood Material (LERMAB), University of Lorraine, Nancy, France

[5] Laboratory of Wood Science - Chemistry & Technology, Department of Natural Environment & Climate Resilience, Democritus University of Thrace, 1 km Drama-Mikrochoriou, 66100, Drama-Greece

* Correspondence: antpap@neclir.duth.gr (A.N.P.); benoit.ndiwe@ensetdouala.net (B.N.)

Abstract: This study explores the extraction of tannins from the barks of four tropical wood species (*Entandophragma candolei, Entandophragma cylindricum, Afzelia africana and Dacryodes klaineana*) and their use in formulating bio-resins. The tannin extraction yield varied between 25 and 40%. The tannins were characterized by 13C Nuclear Magnetic Resonance (13C NMR), Matrix-Assisted Laser Desorption/Ionization Time-Of-Flight (MALDI-TOF) and Thermogravimetric Analysis (TGA). The associated bio-resins, formulated with an *Acacia nilotica* hardener, were evaluated in terms of thermal stability, gel time, and modulus of elasticity. The results reveal significant chemical and thermal variability depending on the wood species. The tannin-based resin from *E. candolei* exhibits the best thermal stability (final residue 36.72% at 600°C), while the one based on *E. cylindricum* shows the best modulus of elasticity (5268 MPa). These tannins represent promising alternatives for bio-based adhesives.

Keywords: tannins; tropical wood barks; bio-based resins; characteristics; applications

1. Introduction

Recent research reveals that interest in the production of bio-polymers, as a sustainable alternative to industrial sector expansion, is driven by environmental concerns related to the use of petroleum-derived products [1]. According to the document titled "Global Market for Bioplastics and Biopolymers 2023," the market for bioplastics and biopolymers is projected to reach $27.3 billion by 2027 [2]. This discovery opens perspectives for the development of new biomaterials derived from responsible natural resource management. Tannins are a category of natural polyphenols, which constitute the second most abundant source in nature, after lignin. These compounds are commonly found in various parts of plants, including fruits, wood, leaves, and bark. Following extensive research, the formulation of tannin bio-resins has been developed. These are commonly used in various industrial sectors, particularly in the manufacture of particleboard and fiberboard. It has been demonstrated that, due to their superior reactivity compared to phenols, these compounds provide

 doi:10.20944/preprints202506.0750.v1

adhesion performance comparable to that of synthetic resins [3,4]. Furthermore, they possess remarkable antioxidant, antibacterial, adhesive, and antimicrobial properties [5]. Moreover, their environmental impact is lower. According to [6] the taxonomy of tannins is based on four categories: condensed tannins (CT), hydrolysable tannins (HT), phlorotannins (PhT), and complex tannins. It has been demonstrated that 90% of the global commercial tannin production consists of CT. These tannins are distinguished by oligomeric structures comprising specific monomers, including catechin, epicatechin, gallocatechins, and epigallocatechins. Currently, global commercial tannin production amounts to approximately 220,000 tons per year. As highlighted by [7], production capacity is unable to meet the growing industrial demand.

Cameroonian forests, covering an area of 22,000 hectares, thus represent 42% of the country's land area. These forests harbor remarkable biodiversity, with a plant diversity of 300 tree species, 80 of which are exploited by logging companies. These activities result in the annual production of over 1.2 million tons of residues, as revealed by studies from [8]. It should be emphasized that the majority of higher plants present in this biomass potentially contain tannins. However, a significant concentration of tannins has been observed in tree bark [9]. Several research works have focused on the extraction of tannins from various Cameroonian tree barks. Within the scope of this research, several species belonging to the *Anigeria spp*. family have been identified, notably *Aningeria superba* [10], *Autranella congolensis*, *Ficus sycomorus* [11], *Ficus platyphylla and Vitellaria paradoxa* [12]. In 2020, the species *Gilbertiodendron dewevrei* was characterized by [13]. Subsequently, Konai [14] studied *Azadirachta indica, Daniellia oliveri* [15]. Wedaïna [8] conducted an in-depth study on *Monopetalanthus durandii*, and focused on *Piptadeniastrum Africanum*. For the same purpose, three other recent plant species have been studied: *Aningeria altissima* [16], *Cissus dinklagei* [17] and *Paraberlinia bifiololata* [18]. These studies led to the conclusion that there is potential for resin production in all the species studied.

The structural diversity and variability in molecular weights of tannins give rise to highly heterogeneous materials. These materials are derived from extracts and frequently lead to non-reproducible processes. Thus, much research utilizes clearly defined and controlled commercial monomers, derived from tannin extraction and purification processes, such as tannic acid, catechol, resorcinol, and catechin [6,19]. However, the use of these monomers can be costly when scaling up the technology, posing challenges for their replacement with alternatives to fossil-based polymers [20]. To make the project cost-effective, it is advisable to use unpurified tannin extracts. Concurrently, a thorough analysis will ensure the consistency of the characteristics of the obtained materials. To achieve this, scientists have employed a plurality of methods for characterizing polyphenols. These approaches include colorimetric, spectrometric, and thermal methodologies. Furthermore, the analysis of formulated resins is primarily conducted through mechanical, thermomechanical, and thermal tests [16,18,21]. This research has highlighted the multiple properties of tannins, which justify their use in various industrial sectors.

Due to their specific characteristics, tannins find applications in different industrial sectors. For example, CT exhibit very high shrinkage temperatures, which facilitates leather tanning [22]. Furthermore, tannins enhance resistance against fungi and termites, thereby offering protection as preservatives [23]. This characteristic gives them a role in the field of preservation [24]. Additionally, tannins are recognized for their ability to improve the durability of wood composites and enhance adhesives, positioning them as materials of choice in the wood and plastic assembly industry [25,26]. Tannins, due to their inhibitory properties, provide protection for metals against corrosion [27,28]. Due to their high aptitude for coagulation and adsorption of methylene blue and heavy metals, tannins possess adsorption characteristics [29,30]. These diverse characteristics underscore the growing interest in tannins as an ecological alternative in industrial sectors. In this context, the present study aims to identify new sources of tropical tannins, evaluate their chemical and thermal properties, and formulate bio-based resins suitable for industrial applications, particularly in the manufacture of panels and ecological inhibitors.

 doi:10.20944/preprints202506.0750.v1

2. Materials and Methods

2.1. Raw Materials

2.1.1. Ecological Hardening Agents

The *Acacia nilotica* hardener was used in the resin formulation. Initially, *Acacia nilotica* exudates were collected from the *Dacheka* forest, located in the Far North Region of Cameroon. After being dried at room temperature for two weeks, they became a soluble powder through grinding and are termed hardener. This process facilitates their packaging and incorporation into the formulation of various resins [16,31].

2.1.2. Tannin Extraction

During the month of November, bark samples were collected from four wood specimens (*Entandophragma cylindricum, Entandophragma candolei, Afzelia africana, and Dacryodes klaineana*) at the logging and wood processing company TRANSBOIS, located in the industrial zone of Douala, in the Littoral Region of Cameroon. Bark collection was carried out selectively, with each tree species being packaged in 50 kg bags. Once collected, a drying process was implemented. The barks were individually air-dried at room temperature (28 °C) for a period of 7 days. Subsequently, they were reduced to very small particles. For the experiment, fine bark particles of each species, extracted from the anhydrous mass, were immersed in an aqueous solution. This solution contained 2% sodium bisulfite and 0.5% sodium bicarbonate. The solid:liquid ratio was 1:6 (v/v). The solution was heated to a temperature of 60 °C and then constantly stirred for four hours. For the study, the solution was filtered through a cotton cloth to obtain a filtered liquid whose color varied depending on the species. The recovered liquid fraction underwent an evaporation process at a temperature of 60 °C, leading to the formation of tannin crystals. For analysis and preservation, it is necessary to have an easier-to-use tannin powder. To achieve this, the crystals were ground into powder using a ceramic mortar [14,16,32]. The extraction yield is then calculated using Equation Eq1:

$$percentage = \frac{m_{\tan nin}}{m_{barks}} \times 100 \quad (1)$$

where: $m_{\tan nin}$ is the mass of the extracted tannin powder

m_{barks} : is the mass of the bark powder taken for extraction

2.2. Tannin Characterization

2.2.1.13. C NMR Analysis

A Nuclear Magnetic Resonance (NMR) spectroscopy analysis was performed on the carbon-13 atom in the liquid phase. The spectra were recorded on a Brüker Advance 400 MHz spectrometer, a state-of-the-art instrument in spectroscopy. Chemical shifts were meticulously calculated relative to tetramethylsilane (TMS), the absolute reference in the field. It is important to note that the spectra manifest at 100.6 MHz. The number of scans and acquisition times were 1.36 seconds and 12,000 seconds, respectively. In the ongoing research on the tannin extract, it was dissolved in a deuterated dimethyl sulfoxide (DMSO-d6) solution, a compound chemically defined as deuterated dimethyl sulfoxide [33].

2.2.2. MALDI-TOF Analysis

In the experiment, 10 milligrams of powder from each of the analyzed tannins were used. For the experiment, the tannin powder, at a concentration of 2 mg/mL, was dissolved in 2 mL of acetone. This solution was then mixed with another solution containing 2,5-dihydroxybenzoic acid and

 doi:10.20944/preprints202506.0750.v1

acetone at a concentration of 10 mg/mL. Finally, ion formation was stimulated by adding sodium chloride (NaCl) to the matrix. Approximately 0.5 liters of the mixed solution was deposited on the Matrix-Assisted Laser Desorption/Ionization Time-Of-Flight/Mass Spectrometry (MALDI-TOF/MS) target and introduced into the spectrometer after solvent evaporation [11,13,32].

2.2.3. Thermogravimetric Analysis of Tannin

In this study, the NETZSCH STA 449 F3 Jupiter analyzer was used to evaluate the thermal stability and decomposition of tannins. In this experimental protocol, a precise quantity of sample powder, with an exact mass between 20 ± 1 mg, was deposited on a platinum platform. Then, the sample was heated from 25 °C to 600 °C, at a heating rate of 20 K.min-1, under a nitrogen atmosphere, thus allowing optimal control of the thermodynamic conditions of the experiment [16,33].

2.3. Resin Characterization

2.3.1. Resin Formulation

An aqueous solution was prepared by mixing 40% tannin powder extracted from each previously mentioned wood species with 40% water and 10% natural exudates of Acacia nilotica. The potential of hydrogen (pH) of the mixture was adjusted to 8 by introducing a 33% sodium hydroxide solution [32,34].

2.3.2. Physical Characterization of Resins: Gel Time

Approximately 10 g of the formulated resin without the addition of a sodium hydroxide (NaOH) solution (33% NaOH) is introduced into a test tube and placed in a water bath, maintained at boiling temperature (100 °C) at normal atmospheric pressure. A metal spring is inserted into the test tube and moved rapidly up and down. The gel time is measured using a stopwatch. The test is performed three times, and the average value is reported by [31]. Then the resin is formulated by adding a sodium hydroxide solution (33% NaOH) to adjust the different pH levels of the mixture. [31].

2.3.3. Thermogravimetric Analysis of Resins

For this study, the NETZSCH STA 449 F3 Jupiter analyzer was used to evaluate the thermal stability and decomposition of the formulated resins. In this experimental protocol, a precise quantity of sample powder, with an exact mass between 20 ± 1 mg, was deposited on a platinum platform. Then, the sample was heated from 25 °C to 600 °C, at a heating rate of 20 K.min-1, under a nitrogen atmosphere, thus allowing optimal control of the thermodynamic conditions of the experiment [33].

2.3.4. Thermomechanical Analysis of the Resin

This method, aimed at characterizing resins, allows for the analysis of interactions between the polymer and various molecules. It also provides data regarding the rigidity of the resin as a function of temperature (Konai et al., 2015a). Sample preparation involves placing 25 milligrams of specifically prepared resin between two smooth plates measuring 21 millimeters in length, 6 millimeters in width, and 1.1 millimeters in thickness. They are then fixed and inserted into a Mettler Toledo 40 Thermomechanical Analyzer (TMA) (MettlerToledo, Zurich, Switzerland). The beech-resin-beech sandwiches were subjected to non-isothermal tests, with a temperature range from 25 °C to 250 °C, at a heating rate of 10 °C/minute. The area covered by the adhesive on the panels is 200 g/m^2. These mentioned plates are decorative beech wood veneers of medium density (0.750 g/cm3), with a thickness of 0.5 mm and a moisture content of 11% (Konai et al., 2021). The samples underwent three-point bending tests over a span of 18 mm, with the application of a force cycle of 0.1/0.5 N and a force cycle of 12 s (6 s/6 s). The mechanical relationship between force and deformation is

 doi:10.20944/preprints202506.0750.v1

$$E = \frac{L^3}{4bh^3} \times \frac{F}{\Delta_{fbois} - \Delta_{fadhesif}}$$

where E: is Young's modulus; L: is the span length; b and h: are the width and thickness of the specimen, respectively; F is the force exerted on the assembly; $\Delta_{f\ wood}$ and $\Delta_{f\ adhesive}$ are the deflections which have been proven constant and reproducible (Das et al., 2020). The tested formulations are therefore those prepared with the different extracted tannins.

3. Results and Discussion

3.1. Tannin Extraction Yield from Different Woods

The analysis of tannin extraction yield from the different wood barks showed that the values range between 25% and 40%. Indeed, *Entandophragma cylindrycum* (SPL) (35%) and *Entandophragma candolei* (KSP) (40%), belonging to the *Meliaceae* family, are characterized by a remarkably high extraction yield. In second place is *Afzelia africana* (DSS) (33%), from the *Fabaceae* family, closely followed by *Dacryodes klaineana* (ADB) (25%), a species from the *Burseraceae* family. It should be noted that tannin extraction was carried out under identical conditions, leading to the deduction that the observed disparities are due to the phenolic compound concentration specific to each bark type. The barks of species belonging to the *Meliaceae* family are distinguished by their scaly texture, the presence of lenticels, and an intense fragrant odor. This is also the case for the *Afzelia africana* species, whose bark has similar characteristics and emits a strong odor of plantain peel. [35]. These specificities could thus justify the superior performance observed in the species of these two groups compared to that of the *Burseraceae*. According to Scalbert [36], the bark of Pedunculate Oak (*Quercus robur L.*) was characterized by a phenolic compound yield of 28.7%. Furthermore, for species such as *Daniellia oliveri, Ficus sycomorus, Butyrospermum parkii*, and *Azadirachta indica*, the results obtained are 29%, 46%, 40%, and 35% respectively [15]. The comparison of these results with those found in this study simply shows that *SPL, KSP, DSS, and ADB* barks are potential sources of polyphenols and tannins.

3.2. Chemical Structures of Molecules Identified in the Samples

The ^{13}C NMR spectra of tannin extracted from wood bark samples of *SPL, KSP, DSS, and ADB* species were subjected to detailed analysis (Figure 1). This study highlighted the presence of various characteristic peaks identified in all examined tannins. The peak at 154 parts per million (ppm) is related to the vibrations of C9, C7, C5 of flavonoids, while the peaks at 144 ppm and 145 ppm represent the vibrations of the C3' and C4' rings in procyanidins [18]. The C1' vibrations of flavonoids are found at peaks 129, 130, and 131 ppm at C4' of prodelphinidins (Njom et al., 2024) . The 116 and 118 ppm peaks reflect the vibrations of the C5' and C2' bonds of procyanidins (Njom et al., 2024) . The C4-C8 interflavonoid linkage is identified between the 108 and 109 ppm peaks depending on the species. The 104 ppm peak observed in *KSP* and *DSS* is the signal related to the C6-C8 linkages of flavonoids [18]. The 80, 81, and 82 ppm peaks indicate the presence of C2 linkages of flavonoids in the *KSP, DSS,* and *ADB* samples. The presence of the C-O-C function is revealed by peaks at 72 ppm in *DSS* and 74 ppm in *KSP*. The peaks at 24 and 11 ppm correspond respectively to free C4 and to the steric –CH2 and aliphatic –CH3 linkages of flavonoids [18].

The tannin spectrum of *KSP* (Figure 1a) showed peculiarities for certain peaks. The peak at 180 ppm is identified as corresponding to the –COOH function linked to a non-aromatic ring, while the peaks at 173 ppm and 168 ppm are respectively associated with the –C=O of an aliphatic and cyclic ester. The peak at 145 ppm is indicated by the C5 site of the furanic acid, prieuridine, and azadiradrone rings. This observation is supported by the emergence of the peak at 134 ppm, which relates to the C2 vibration of these recognized compounds. The peak at 74 ppm concerns the C-O bond, linked to molecules such as aziridones and flavonoids. Furthermore, the existence of

 doi:10.20944/preprints202506.0750.v1

characteristic peaks of prieuridine is also observed. The peak at 37 ppm is linked to catechinic acid, while the peak at 30 ppm concerns the C6 bond of aziridone. Furthermore, the tannin revealed new elements such as furanic acid, which belongs to the amino acid category, as well as prieuridine and aziridone, classified as alkaloids.

Furthermore, the analysis of the tannin spectrum of *SPL* (Figure 1c) allowed for the identification of specific peaks. In particular, the peak at 181 ppm is linked to the –COOH connection of strongly protonated acetic acid, derived from hemicelluloses. Indeed, this band should appear at 178 ppm, but its identification at 181 ppm indicates degradation of hemicelluloses during extraction. This variation may also be due to the presence of glucuronic or galacturonic acids, resulting from carbohydrate degradation, forming hemicellulose segments. Furthermore, the value of 147 ppm indicates the presence of –COOH, while 168 ppm is related to the –COOH of gallic acid. The peak at 74 ppm is characteristic of sugar oligomers, while the peak at 36 ppm corresponds to the carbon atom vibrations of Tau-Cadinol, alpha-copaene, and gamma-cadinene. The peak at 30 ppm is linked to the C4 of flavonoids and the CH2 groups of Tau-Cadinol, while the peak at 18 ppm represents the CH3 groups of Tau-Cadinol, alpha-copaene, and gamma-cadinene.

Regarding the tannin profile of *DSS* (Figure 1d), the notable observed peaks are at 174 ppm; 56 ppm; 40 ppm; 36 ppm and 22 ppm. The peak at 174 ppm indicates the presence of substances such as eriodictyol and methoxyeriodiol, which are sterols. The peak at 56 ppm corresponds to the methyl group –OCH3 found in methoxyeriodictyol. The peak at 40.9 ppm is associated with the C3-H group of eriodictyol. The peaks at 36 ppm and 22.7 ppm indicate the presence of eriodictyol and methoxyeriodictyol, either alone or in combination with other flavonoids. Regarding the flavonoid tannin peaks, particularly those of C5, C7, and C9, which are generally located at 154 ppm, it was noted that the peak intensity is more pronounced. This is because it is an isolated peak for three carbon atoms, rather than the usual two peaks. The peak at 144 ppm indicates the highest concentration noted for C3' and C4' compounds. The C1 of flavonoids is associated with a value of 129.7 ppm. The peak at 116 ppm indicates the highest concentration of C2' and C5' for flavonoids such as catechin or fisetinidin (hemicellulose residues).

Furthermore, the 13C NMR spectrum analysis of tannin from *ADB* (Figure 1b) reveals the following distinct peaks: 180; 174; 73; 39; 27; 19 and 14 ppm. The peak at 180 ppm is associated with the –COOH group of protonated acid, originating from hemicellulose degradation. The peak at 174 ppm is linked to the C=O group of xanthones, while the peak at 73 ppm concerns carbohydrates, related to hemicellulose fragments. Finally, the peak at 55 ppm is associated with a –CH3 group linked to an O. The values of 39.8, 24.7, 19.9, and 14.8 ppm are associated with the compound's beta-amyrin, quercetin 3-O-alpha-L-rhamnoside, or the methyl ester of trihydroxy olean-12-en-28-oic acid. The identification of various signals related to phenolic hydroxyl groups confirms the condensed nature of each tannin examined [37].

 doi:10.20944/preprints202506.0750.v1

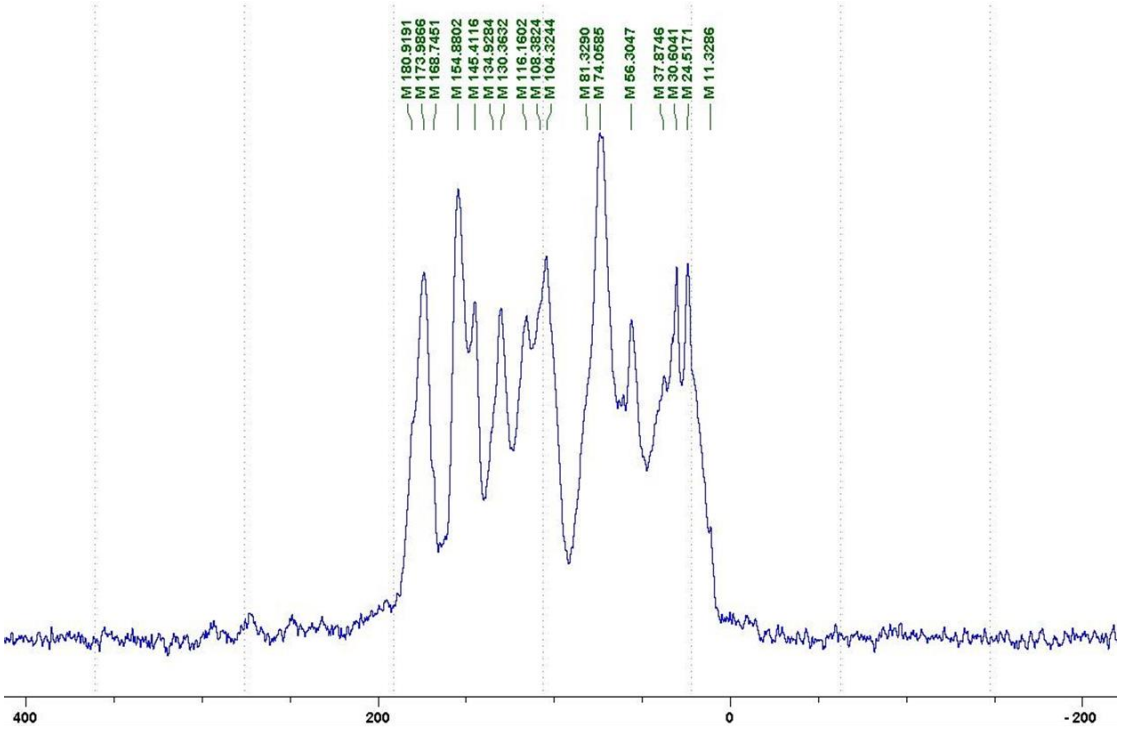

(a)-*Entandophragma candolei*

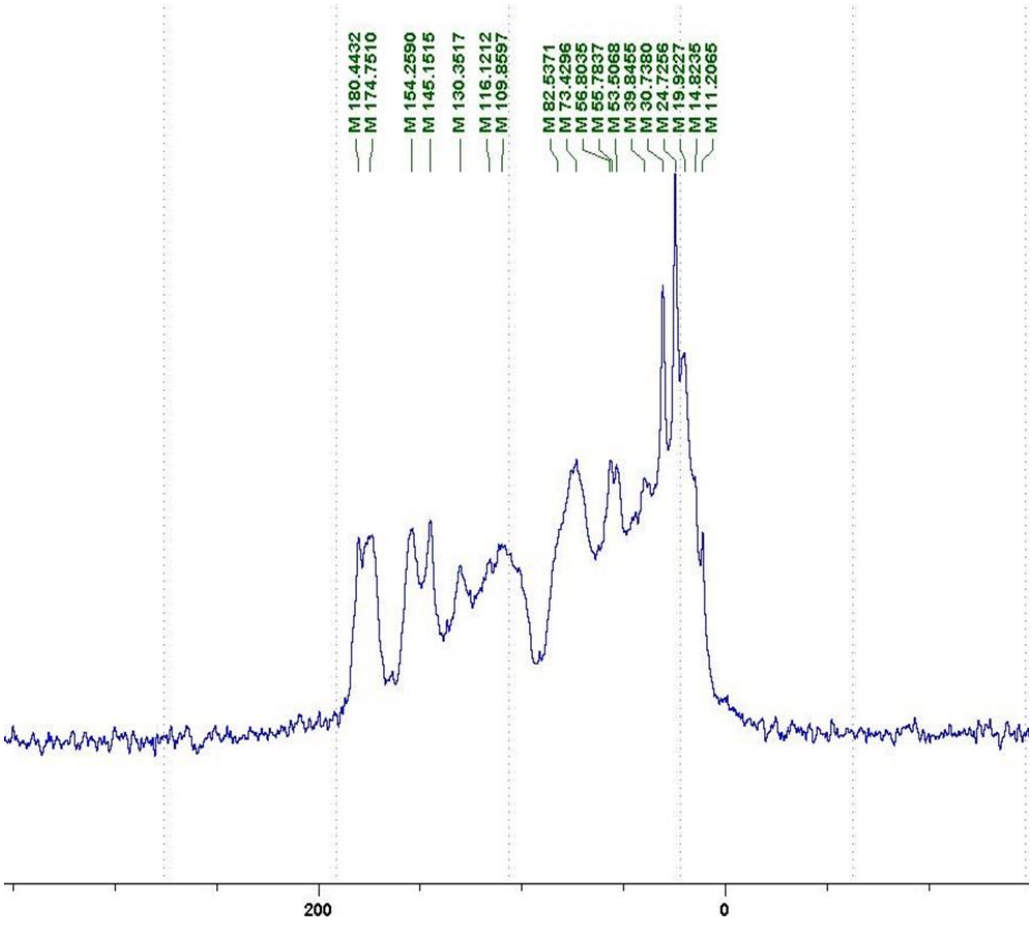

(b)-*Dacryodes klaineana*

 doi:10.20944/preprints202506.0750.v1

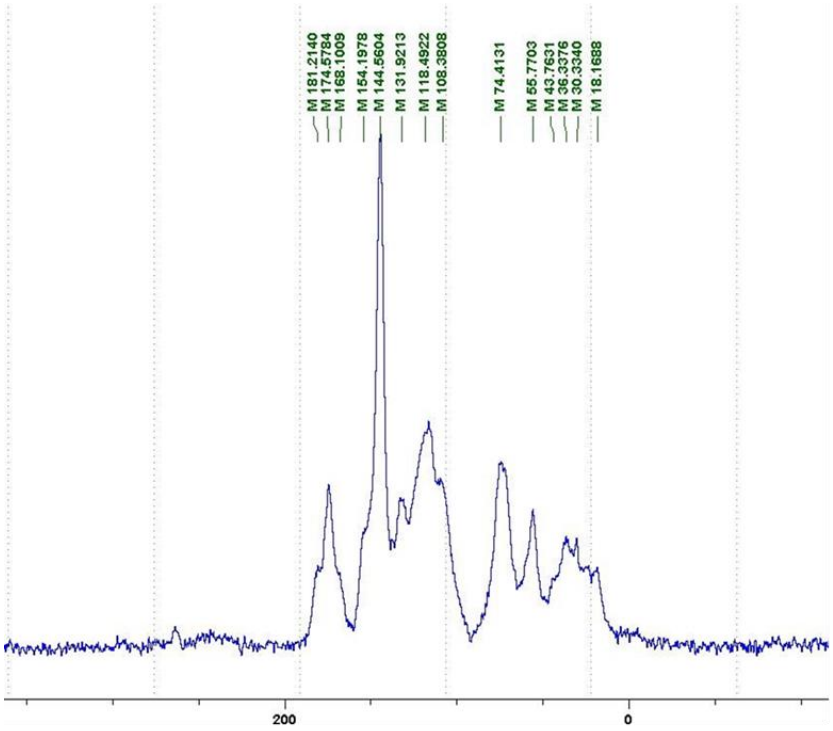

(c)-Entandophragma cylindrycum

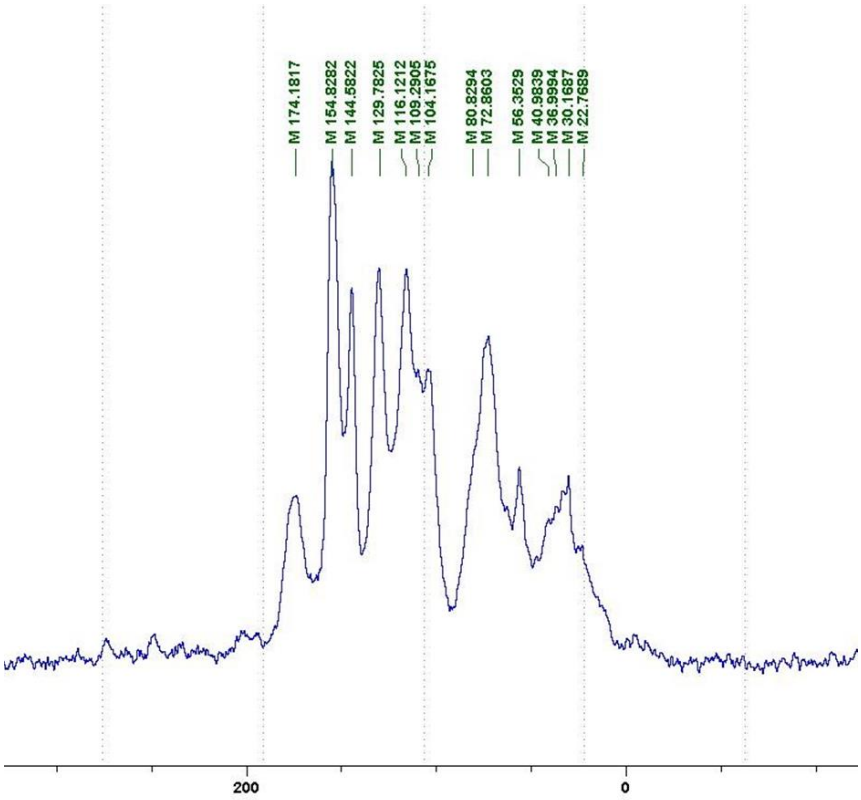

(d)-Afzelia africana

Figure 1. ^{13}C NMR spectra of the samples of the 4 analyzed tannins.

 doi:10.20944/preprints202506.0750.v1

3.3. Structural Determination of Molecules from Different Tannin Samples

MALDI-TOF analyses of tannin from the wood barks of *SPL, KSP, DSS, and ADB* species show similar and distinct oligomers. Let us present the main oligomers identified in each tannin sample.

For the *DSS* sample, the peak at 177 Da refers to a molecule Syringaldehyde fragment with loss of 5xH found among forestry by-products in this sample [38]. 192 Da corresponds to protonated gallic acid. At 199 Da, we have the new molecule (177) bound to Na^+. 274 Da corresponds to the structure of fisetinidin detached from Na^+. The peak at 309 Da corresponds either to deprotonated Eriodictyol bound to Na+, or to protonated anthraquinone bound to Na+ (the structures(b)). 326 is protonated Eriodictyol or a labile H of the –OH functional group has been replaced by the –CH3 alkyl group (structure(c). 352 Da = no Na+, deprotonated. This is a fragment of a flavonoid dimer like the structures at 193 Da above that were isolated in previous analyses. 449 Da corresponds to the Catechin-3xH dimer linked to glucose [39]. The peaks 553, 575, and 577 Da correspond respectively to the Robinetinidin-Trihydroxyflavan $+7H^+$ dimer and deprotonated Gallocatechin ($-H^+$ for 575 Da and $-3H^+$ for 577 Da (Athomo et al., 2018). The peaks at 581.5 and 584 Da correspond respectively to fisetinidin-eriodictyol and fisetinidin-catechin dimers, all bound to Na^+. The 625 Da peak corresponds to the Isoquercetin gallate +5H+ peak, and 709 Da corresponds to the trimer of Fisetinidin, Gallocatechin, and Gallic acid [39]. 758 Da corresponds to the trimer of Gallic acid, Trihydroxyflavan, and glucose hydrate. The peaks 772 Da protonated with Na^+, 801 Da without Na+, indicate the presence of a trihydroxyflavan and fisetinidin dimer ($-8H^+$ for 772 Da) and ($-2H^+$ for 801). 846 Da corresponds to a fisetinidin-catechin-eriodictyol trimer, deprotonated without Na+. 889 Da is a catechin trimer, bound to Na+.

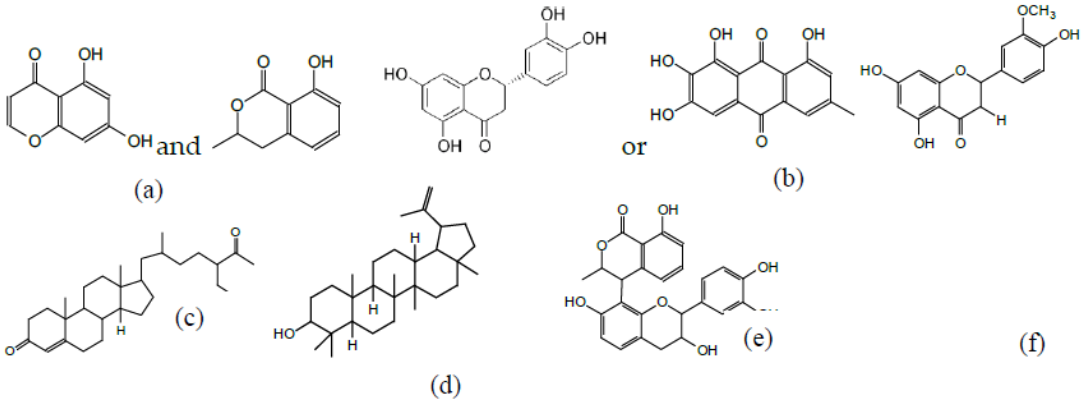

For the *ADB* tannin, the following peaks were interpreted: 137 Da without Na^+, 159 Da with Na^+. These correspond to the following Terpenes: (1) Alpha-Thujene; (2) alpha-pinene; (3) camphene; (4) Sabinene; (5) beta-pinene; (6) alpha-phellandrene; (7) alpha-terpinene; (8) gamma-terpinene. 177 Da bound to Na^+ corresponds to the following terpenic structures: (9) 1,8-Cineole; (10) *cis*-Sabinene hydrate; (11) Terpinen-4-ol; (12) alpha-terpineol (g). The 192.8 Da peak is that of gallic acid bound to Na^+. 196 Da corresponds to Xanthone in the absence of Na^+. 326 Da = with Na^+, either(a) deprotonated delphinidin, or(b) 9-(4-methoxyphenyl) xanthene (second most probable hypothesis) or both(h). 449 Da = with Na^+, beta-amyrin; or without Na^+ quercetin 3-O-Alpha-L-Rhamnoside(i). 509 Da = with Na^+, deprotonated, methyl ester of 2,3,23-trihydroxyolean-12-en-28-oic acid new molecule(j). 575-577 Da = no Na^+, Sitosterol-3-O-Beta-D-glucopyranoside sterol, (576 Da), protonated (577 Da) and deprotonated (575), and/or, or both catechin dimers, deprotonated (577) no Na^+(k). 585 Da corresponds to a non-protonated catechin-fisetinidin dimer without Na^+. The 595, 619 Da peaks protonated bound to Na^+ correspond to the catechin-delphinidin dimer; 611 Da without Na^+, protonated corresponds to the delphinidin-delphinidin dimer. 729Da corresponds to a fisetinidin dimer without Na+ bound to glucose molecules. 745 Da is a Catechin-Fisetinidin dimer bound to glucose molecules associated with Na+ and deprotonated. 760Da is a catechin dimer attached to glucose molecules. 921Da is a delphinidin-delphinidin-catechin trimer attached to Na+.

 doi:10.20944/preprints202506.0750.v1

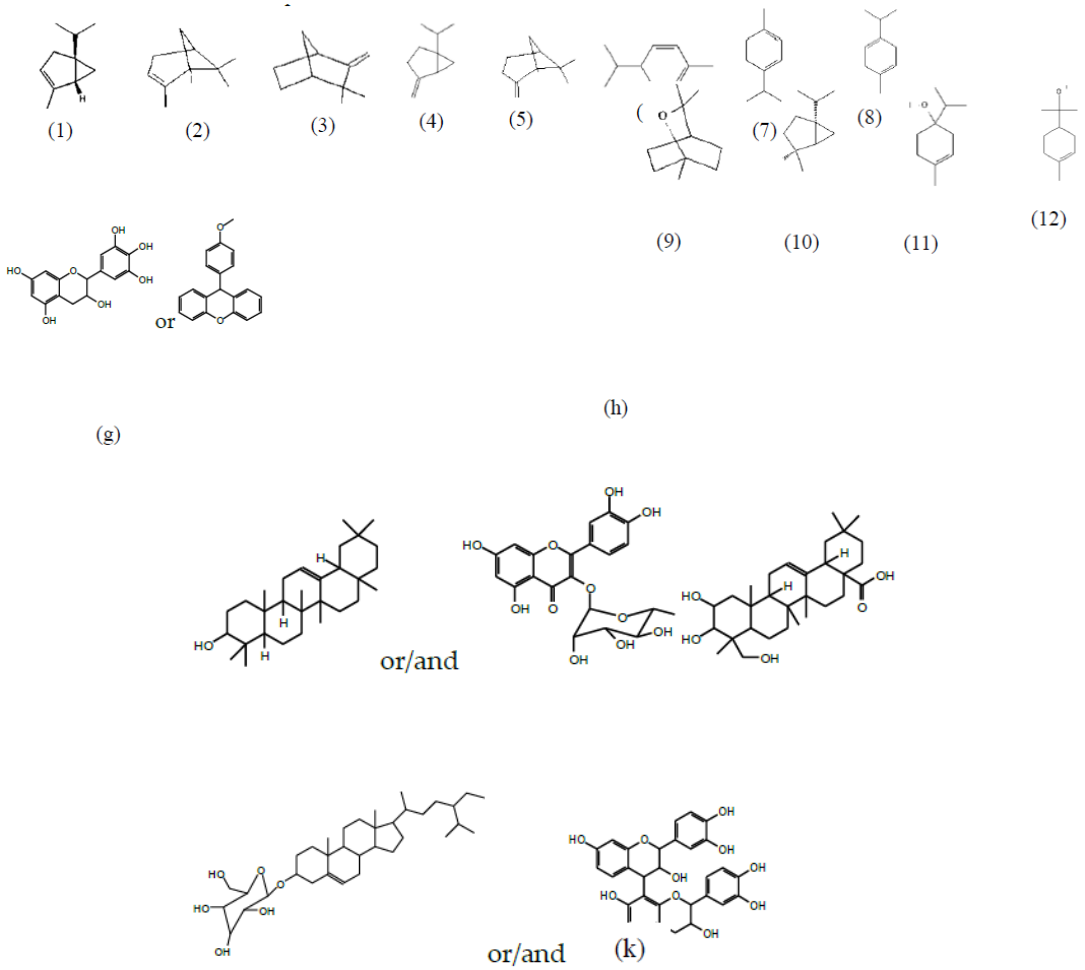

The following peaks allowed for the interpretation of the MALDI-TOF spectrum of *SPL*. The 192Da peak corresponds to gallic acid bound to Na^+ [8], 204 Da = no Na^+, small peak of alpha-copaene (1l) or gamma-cadinene (2l), or both mixed(m). 223 Da corresponds to Tau-Cadinol, protonated and bound to Na^+(n). The 273 Da peak is that of fisetinidin**,** without Na^+. 309 Da no Na^+, protonated delphinidin (307 Da) (1), or with Na^+, deprotonated eriodictyol (310) (2) or both(n). 405 Da is the Cadinol peak attached to glucose and Na+. The 443 Da peak is that of Catechin gallate, without Na^+. 493 Da corresponds to protonated delphinidin bound to glucose and Na^+. 501 Da is the peak of fisetinidin esterified by tau cadinol without Na^+,(o). 549 Da is a deprotonated fisetinidin-fisetinidin dimer without Na^+. 577 Da is either a deprotonated delphinidin-fisetinidin dimer without Na+, or/and a catechin-catechin dimer. The 581, 595 Da peaks correspond respectively to the deprotonated catechin-fisetinidin dimer without Na^+ and the delphinidin-catechin dimer without Na^+ [8], protonated, or of fisetinidin-$(glucose)_2$ without Na^+. The 625-627 Da peak corresponds to delphinidin-$(glucose)_2$ without Na+ [8]. 713 Da corresponds to the fisetinidin-fisetinidin-glucose structure, protonated without Na^+ [8]. 757 Da corresponds to the catechin-delphinidin-glucose structure without Na^+ [8]. 765 Da is delphinidin-fisetinidin-glucose, protonated bound to Na^+. 889 Da corresponds to a catechin trimer, bound to Na^+. 1175 Da is a glucose heptamer bound to Na^+ or of glucose-mannose, which is a hemicellulose fragment. 2015-2016 Da is a catechin heptamer, in the absence of Na+. 2306 Da is a catechin octamer, without Na+.

Preprints.org (www.preprints.org) | NOT PEER-REVIEWED | Posted: 10 June 2025 doi:10.20944/preprints202506.0750.v1

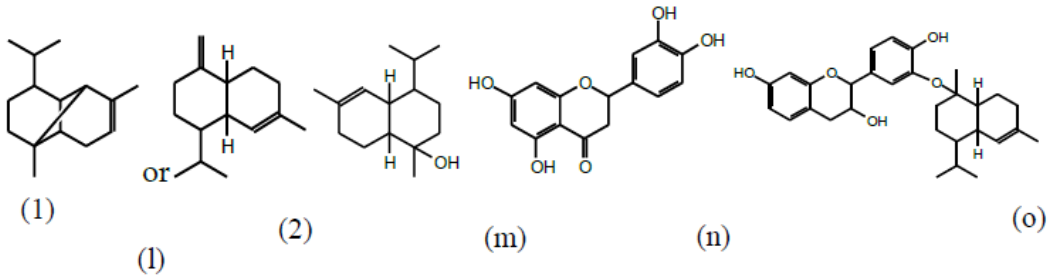

The following peaks caught our attention in the interpretation of the MALDI-TOF spectrum of *KSP*; the 199Da peak is that of N-methyl 5-dihydroxypipecolic acid (p) (Nga et al., 2024a). 231 Da is attributed to deprotonated Chalcone; 273 Da is fisetinidin, without Na+; 295 is attributed to the protonated catechin monomer. The 326 Da peak is that of protonated Eriodictyol (c). 377Da corresponds to Dihydroxyflavan-3-(3,4-dihydroxy)-benzoate [38]. 413Da is attributed to the deprotonated Chalcone dimer [8]; 449 Da corresponds to the dihydroxypipecolic acid trimer [18]. (q). The peak at 493 corresponds to the Quercetin-gallate monomer bound to Na+. 575 Da corresponds to the Gallocatechin dimer –Na+, deprotonated. 669 Da is the pentamer of N-methyl 4-hydroxypipecolic(r) (Nga et al., 2024a). 753 Da corresponds to catechin-delphinidin-glucose, without Na+, deprotonated [8]. The 827Da peak is that of the deprotonated Chalcone tetramer [8]. The peak at 1579Da is that of Fisetinidin/ trihydroxyflavan, protonated [38].

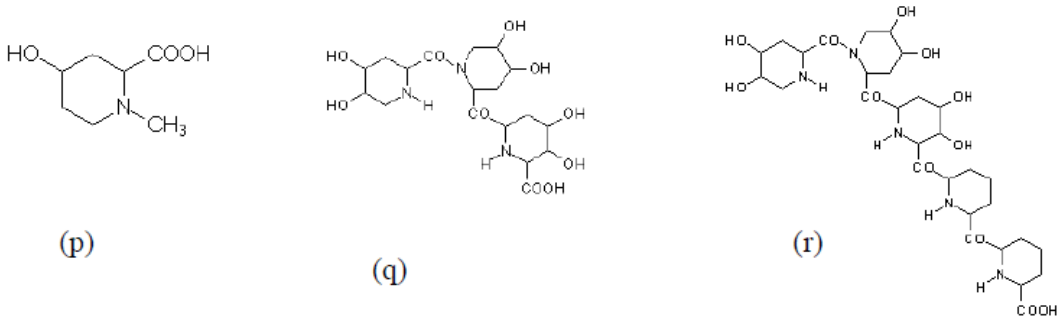

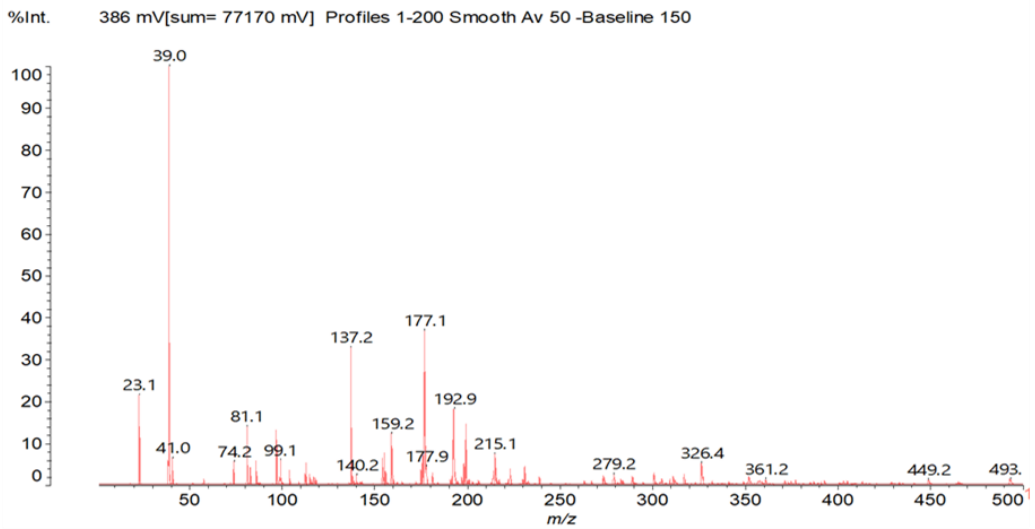

Dacryodes klaineana

Preprints.org (www.preprints.org) | NOT PEER-REVIEWED | Posted: 10 June 2025 doi:10.20944/preprints202506.0750.v1

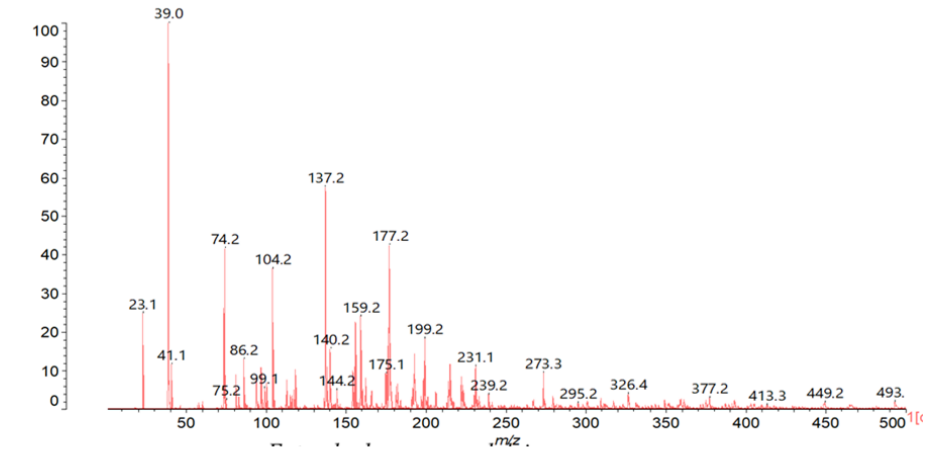

Entandophragma candolei

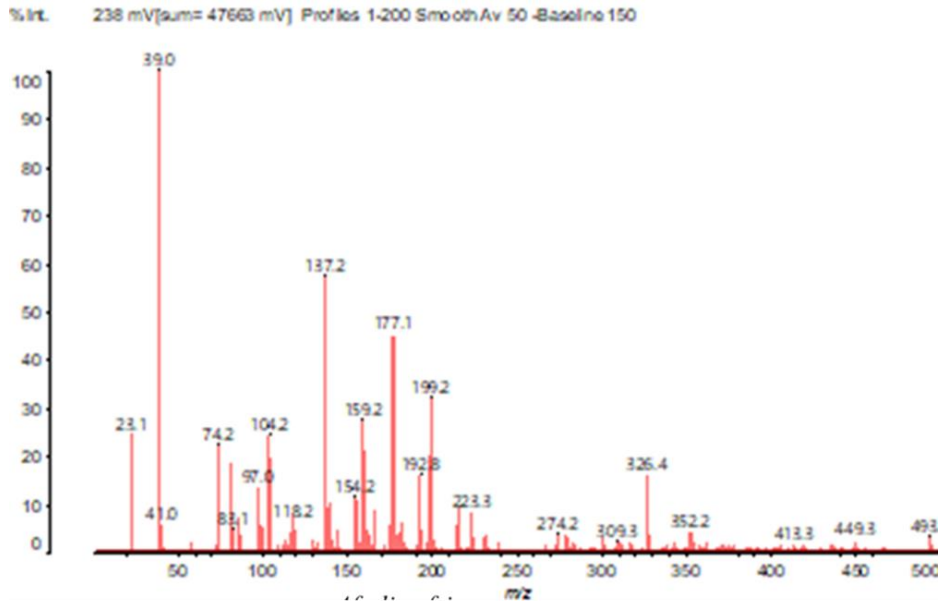

Afzelia africana

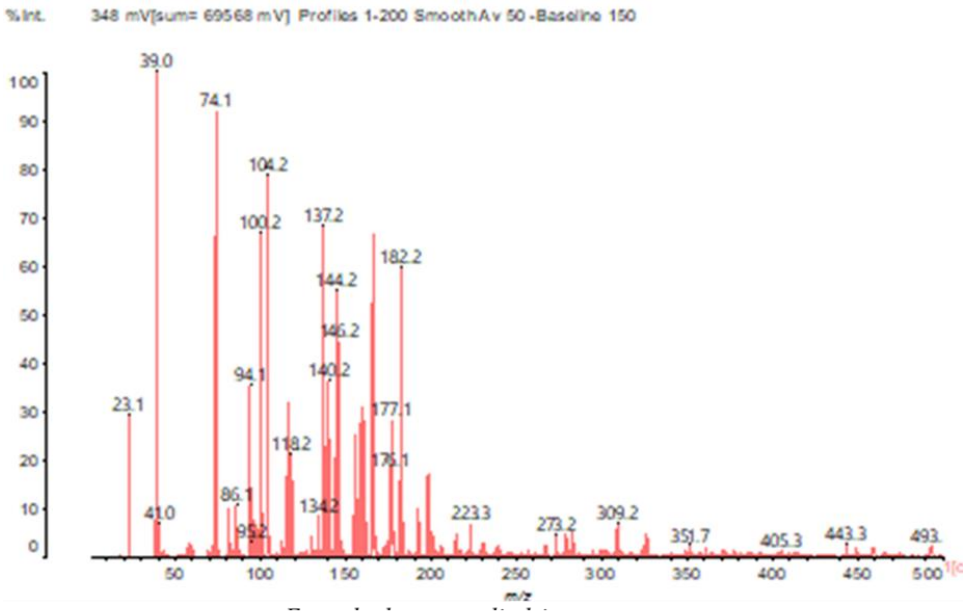

Entandophragma cylindrycum

Figure 2. MALDI-TOF spectrum between 0-500Da.

 doi:10.20944/preprints202506.0750.v1

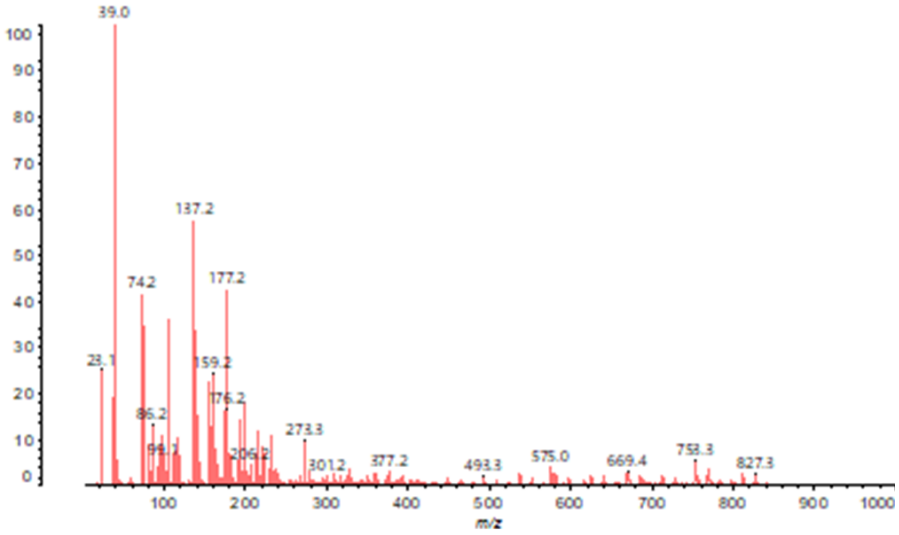

Entandophragma candolei

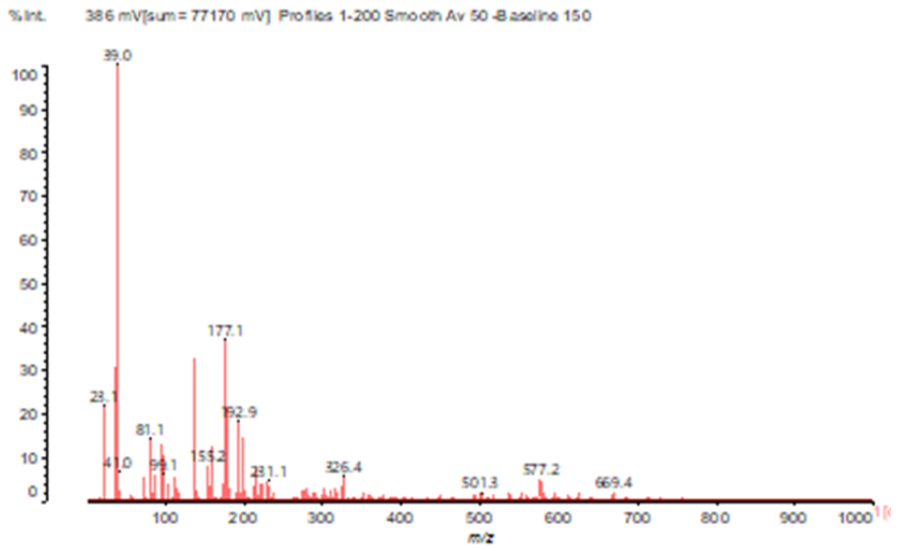

Dacryodes klaineana

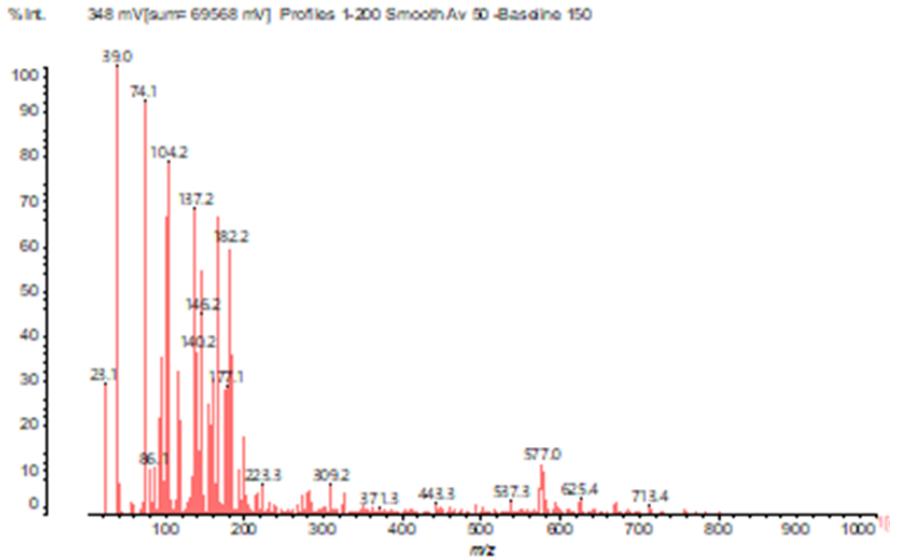

Entandophragma cylindricus

Preprints.org (www.preprints.org) | NOT PEER-REVIEWED | Posted: 10 June 2025 doi:10.20944/preprints202506.0750.v1

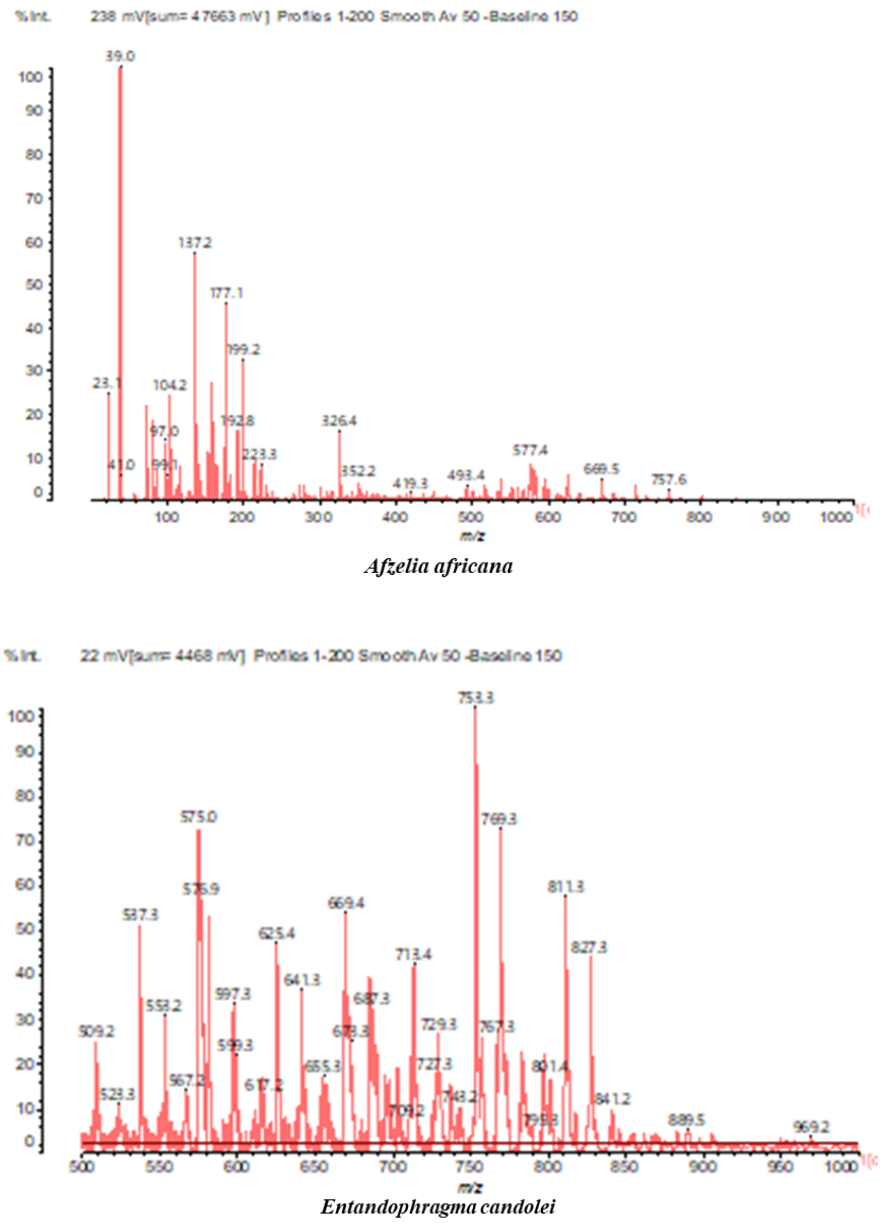

Figure 3. MALDI-TOF spectrum between 100 and 1000 Da.

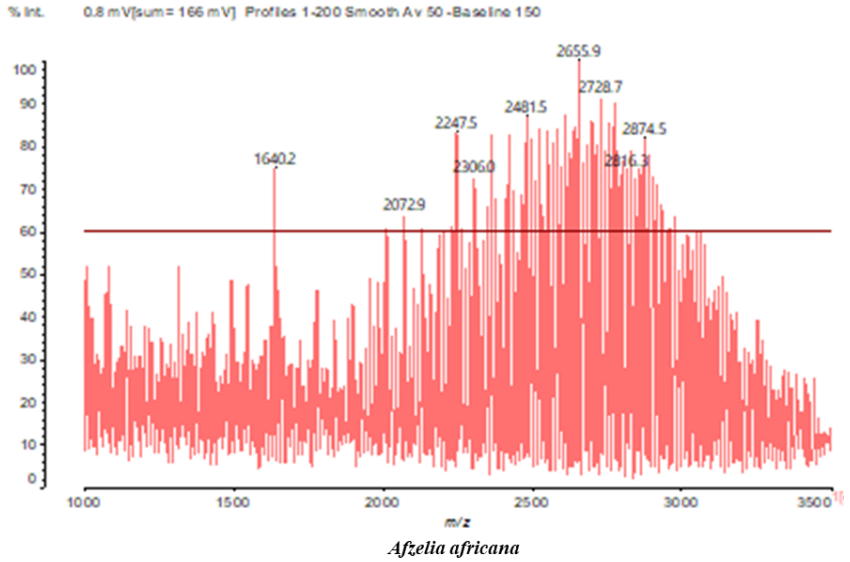

 doi:10.20944/preprints202506.0750.v1

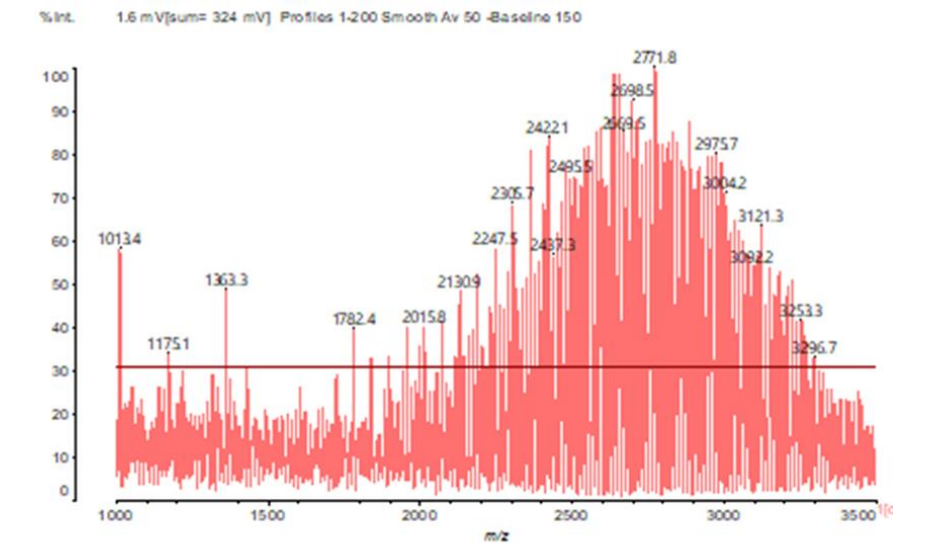

Entandophragma cylindricus

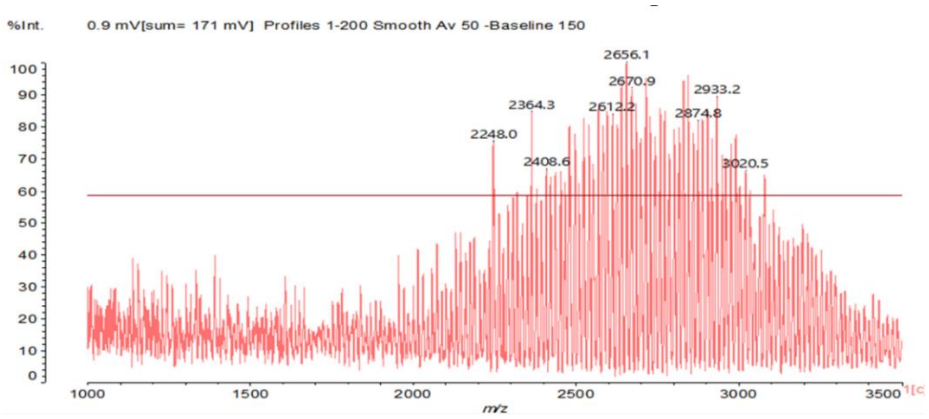

Dacroydes klaineniana

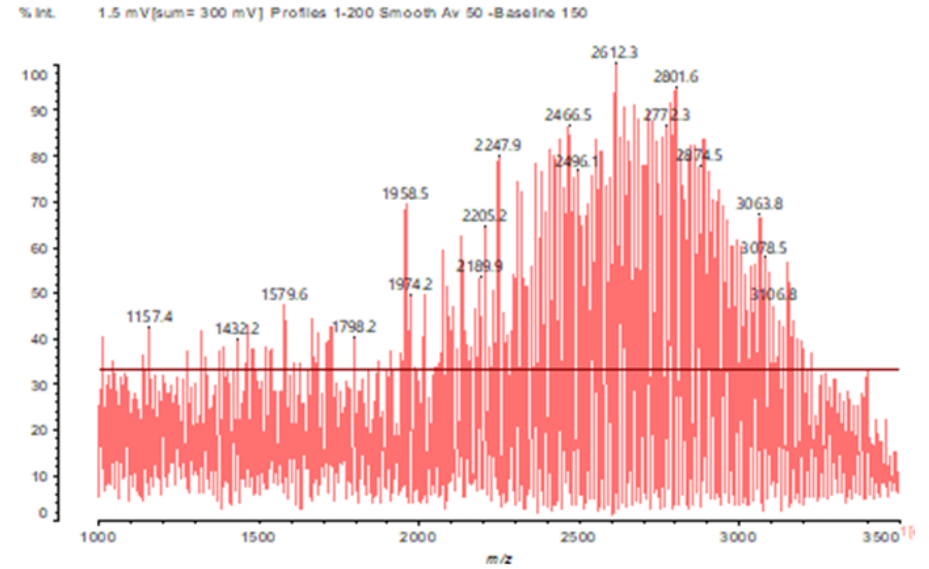

Entandophragma candolei

Figure 4. MALDI-TOF spectrum between 1000-3500Da.

 doi:10.20944/preprints202506.0750.v1

3.4. Thermogravimetric Analysis of Tannins and Resins

The TG/DTG curves of crude tannins *ADB*, *DSS*, *KSP*, and *SPL*, as well as those of the tannin resins *ADBN*, *DSSN*, *KSPN*, and *SPLN* (Figures 5–8) under nitrogen, allowed for the identification of the main stages of the thermal decomposition mechanism of the adhesives.

The analysis of *ADB* tannin (Figure 5b) revealed three distinct phases: a first phase of water and volatile evaporation at a temperature of 95°C, followed by a second phase of heteropolysaccharide and glycosidic bond degradation at a temperature of 275°C. A third phase of polyphenolic structure breakdown was then observed at a temperature of 525°C. At 600°C, a high char yield (45.05 %) [37] is obtained, probably due to the aromatic nature of the tannin and the presence of minerals such as silica (Santoso et al., 2016; Amari et al., 2021). Concurrently, the analysis of the *ADBN* resin (Figure 5a) reveals an initial water loss at 95°C, volatilization of small molecules at 275°C, and major degradation beyond 600°C. The analysis of the final residue (32.41 % at 625°C) allows for the conclusion of the presence of a complex polymer structure. The incorporation of the hardener into the composition of the studied material has the effect of increasing thermal stability, reducing low-temperature losses, and promoting effective crosslinking.

Furthermore, the thermal study of the *DSS*/*DSSN* pair reveals notable disparities in terms of stability. The *DSSN* resin (Figure 6a) undergoes four degradation phases. The first significant magnitude corresponds to a loss of 40.80 % after 30 minutes of exposure. Continuing this observation, it is noted that additional reductions are observed at 45 and 60 minutes, leading to a total loss of 68.23 %. Indeed, the *DSS* tannin (Figure 6b) exhibits superior thermal resistance, characterized by more gradual losses, reaching 56.82 % and a more substantial final residue (43.18 %) [40,41]. These results suggest that the crude *DSS* tannin exhibits superior thermal stability compared to its *DSSN* resin. However, the introduction of the *Acacia nilotica* hardener induces intense crosslinking, but it also promotes the formation of bonds that are more fragile when exposed to heat. Thus, the choice of hardener must be meticulously adapted according to the final application.

Furthermore, the *KSP* tannin (Figure 7a) exhibits a moderate initial loss of 7.08 %, followed by two major degradations at 41.72 % and 29.47 %, leading to a residue of 30.80 %, a sign of a highly refractory structure. Moreover, the *KSPN* resin (Figure 7b) undergoes a more complex degradation, in several phases (7.93 %, 36.71 %, 15.45 %, and 7.41 %), due to the progressive breaking of bonds between tannin and hardener. The final residue of 36.72 % is a sign of a more advanced decomposition of the polymer matrix [40,41]. These discrepancies highlight the determining impact of the crosslinking agent, in this case *Acacia nilotica*, on thermal stability. The modification of the polymer network structure induces a more elaborate architecture of the resin. However, we have a more elaborate polymer network and better crosslinking of the KSPN resin during the thermal decomposition process.

The analysis of the *SPL* tannin [40,41]) reveals the presence of five distinct stages of thermal decomposition. The two highest peaks are attributable to water evaporation and the degradation of light elements, while the next three peaks are correlated with the progressive degradation of the polyphenolic structure, resulting in a significant final loss of 7.94 %. The observation of a secondary exothermic peak supports the hypothesis of partial combustion of carbonaceous residues [41]. Data analysis reveals that the final residue of 35.70 % indicates thermal stability deemed satisfactory [42].

In contrast, the *SPLN* resin (Figure 8b) exhibits a more crosslinked structure, but lower thermal stability, with three main degradation phases and a lower residue (21.84 %). An unusual exothermic peak observed on the *SPLN* curve could indicate a calibration error or a secondary recombination phenomenon. It emerges from the study conducted that, in general, the *SPL* tannin exhibits superior thermal resistance. This property is attributable to the aromatic nature of the tannin structures. In contrast, the resin, despite more significant degradation, exhibits homogeneous crosslinking.

Table 1 summarizes the performance of each of the materials studied in this research. It appears that the *KSPN* resin exhibits the best thermal stability compared to all other formulated resins. This observation highlights the positive impact of the hardener on the thermal stability of the formulation, but an optimization of the formulations would be necessary for a better evaluation of the resins. In

 doi:10.20944/preprints202506.0750.v1

general, crude tannins (*ADB, DSS, SPL*) perform better than their associated resins, benefiting from better heat resistance. Among all the materials studied, *ADB* tannin stands out for its optimal thermal stability.

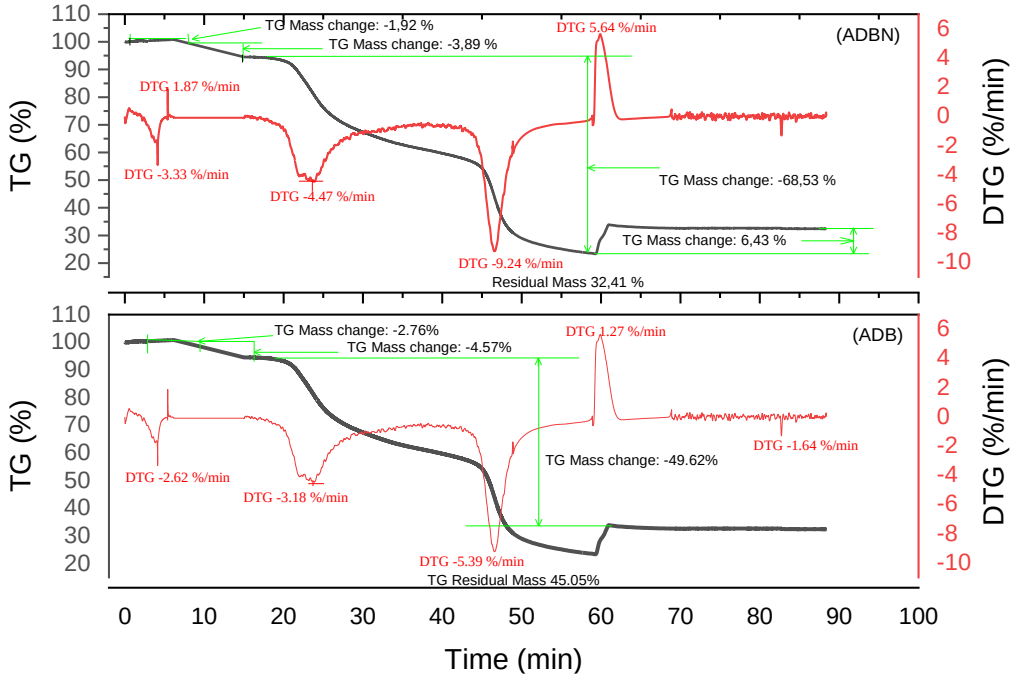

Figure 5. Curves TGA of ADBN and ADB (a:up ; b:bottom).

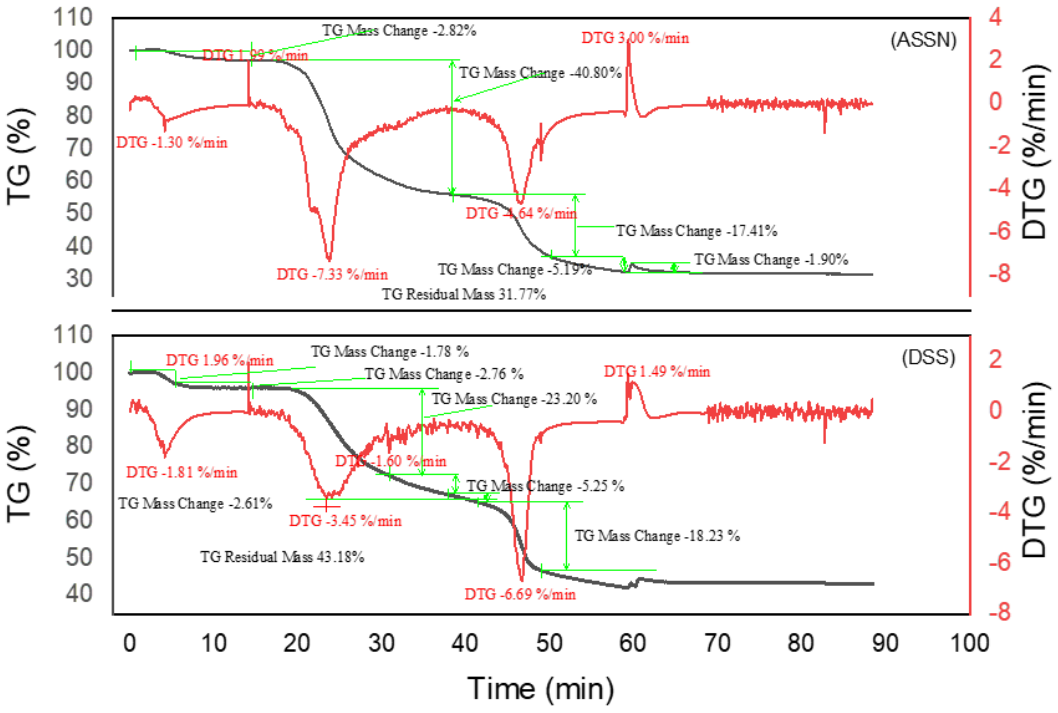

Figure 6. Curves TGA of DSSN and DSS (a:up ; b:bottom).

 doi:10.20944/preprints202506.0750.v1

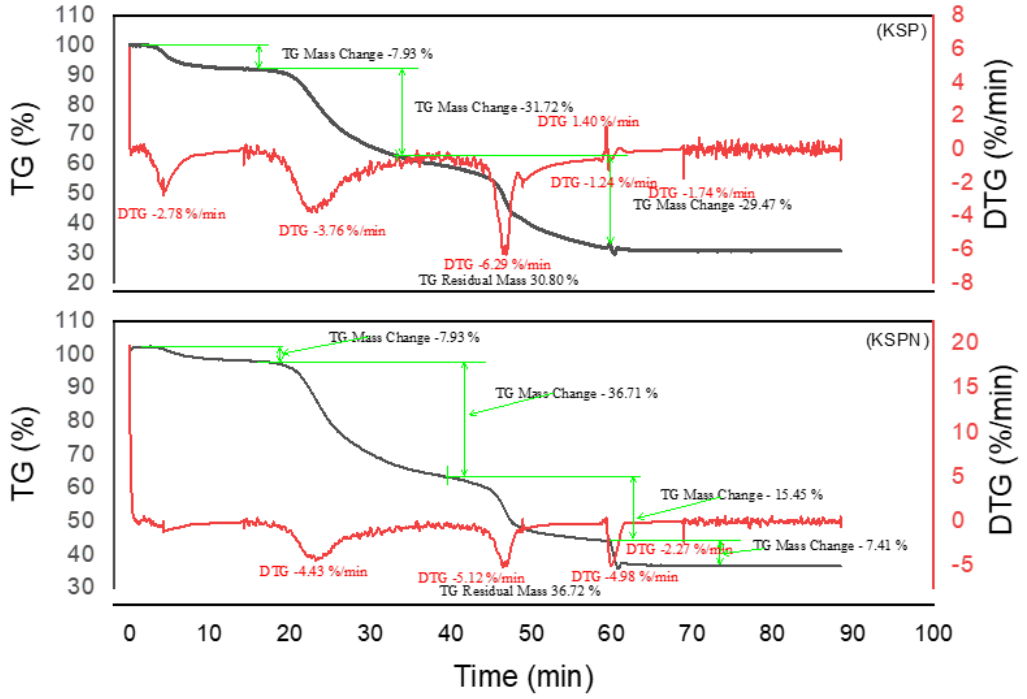

Figure 7. Curves TGA of KSP and KSPN (a:up ; b:bottom).

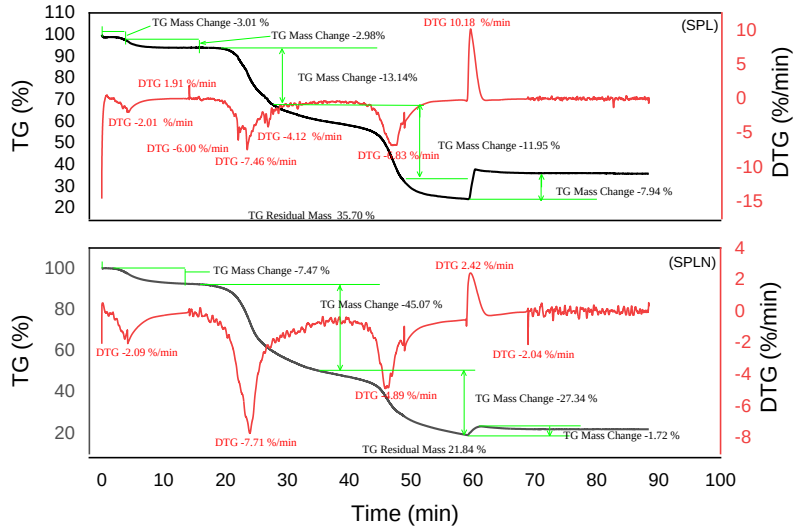

Figure 8. Curves TGA of SPL and SPLN (a:up ; b:bottom).

Table 1. Thermogravimetric comparison of crude tannins and their resins formulated with Acacia nilotica.

Material	Decomposition phases	Final residue (%)	Thermal stability	Remarks	Best performing material
ADB	**3**	**45,05**	High	Good stability up to 600 °C, high carbon retention	*****
DSS	**4**	43,18	High	Progressive decomposition, better heat resistance	

 doi:10.20944/preprints202506.0750.v1

SPL	**5**	35,70	Good	Good thermal resistance, partial combustion	
KSP	**3**	30,80	Average	Marked thermal decomposition, notable loss	
ADBN	**3**	32,41	Average	Successful crosslinking but average thermal stability	
DSSN	**4**	31,77		Thermolabile bonds, significant thermal loss despite crosslinking	
SPLN	**3**	21,84	Low	More homogeneous network but low residue	
KSPN	**4**	**36,72**	Good	More elaborate polymer network, better crosslinking	****

3.5. Resin Gel Time

Tables 2 and 3 show the time required for the tannin resin to become rigid when combined with an *Acacia nilotica* hardener. It appears that, at a natural pH (6.4 and 6.7), the average curing time of *Entandophragma candolei (KSPN)* resin is 1887 seconds, that of *Afzelia africana* (*DSSN*) is 1880 seconds, that of *Dacryodes klaineana* (*ADBN*) is 1746 seconds, and that of *Entandophragma cylindricum* (*SPLN*) is 1811 seconds. It should be noted that this duration is considerably reduced when the pH is modified (11.2-11.8) through the incorporation of a 33% sodium hydroxide solution. Figure 9 shows the average curing time for each type of resin as a function of pH. The *KSPN* resin cures in 448 seconds, that of *SPLN* in 431s, while the *DSSN* resin requires 430 seconds and that of *ADBN* 427 seconds. We observed that the resin curing time decreased considerably when treated with sodium hydroxide. Indeed, sodium hydroxide serves to increase the hydroxyl functions in the tannin structure, i.e., its reactivity, and consequently improves the gel time [13]. Although synthetic resins have a shorter curing time than natural resins, the reactivity of the corrected resins formulated in this study remains interesting compared to others. This is the case for resins formulated with *Mimosa* tannin and hexamine (600s), and *Mimosa* tannin and lignin in proportions of 90/10, 80/20 (623s, 620s) [43]. Furthermore, it has been shown that formaldehyde resins had a very short gel time, approximately 50 seconds at 100 °C for pure *Maritime pine* tannin hardened with paraformaldehyde [31]. Compared to the longer gel time of the resin formulated in this study, we can therefore say that our resin does not contain a significant amount of aldehyde [31], thus being environmentally responsible.

Table 2. Measurement of resin gel time at natural pH.

Trials	**1**	**2**	**3**	**pH**
Species	**Time in second(s)**			
Entandophragma candolei	1787	2188	1686	6,5
Afzelia africana	1810	1985	1755	6,7
Dacryodes klaineana	1692	1746	1802	6,4
Entandophragma cylindrycum	1929	1756	1750	6,6

Table 3. Measurement of resin gel time after addition of 33% concentrated sodium hydroxide.

Trials	**1**	**2**	**3**	**pH**
Wood species	**Time in second(s)**			
Entandophragma candolei	440	435	468	11,2

 doi:10.20944/preprints202506.0750.v1

Afzelia africana	430	425	435	11,6
Dacryodes klaineana	432	426	422	11,3
Entandophragma cylindrycum	429	436	430	11,8

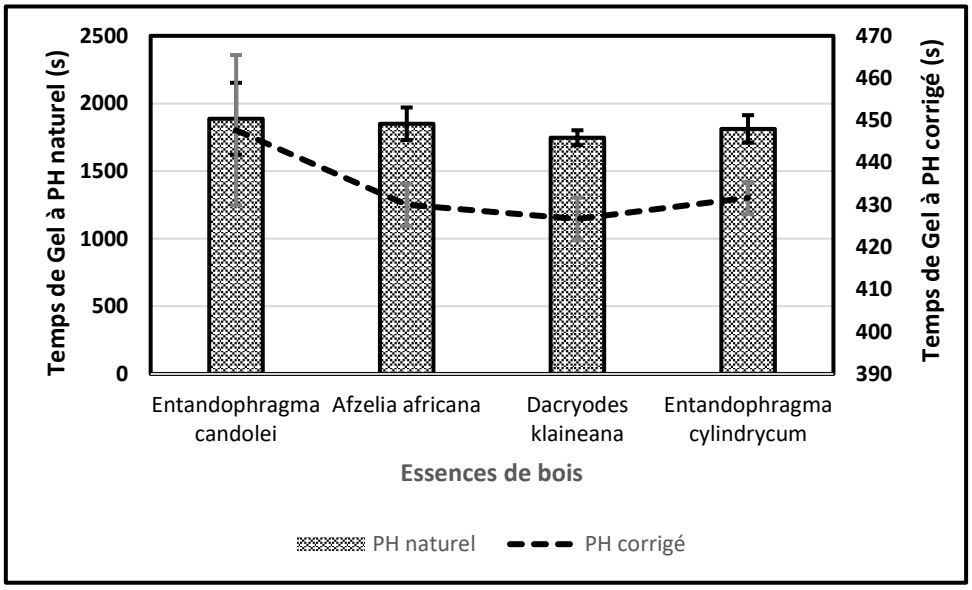

Figure 9. Influence of pH in resin formulation.

3.6. Thermomechanical Analysis of the Resin

The thermograms expressing the Modulus of Elasticity (MOE) as a function of temperature of the different formulated resins are given in Figure 9. It is noted that the resin formulated with *SPLN* tannin has the highest modulus of elasticity (5267MPa) compared to other formulations. Next is the resin based on *ADBN* tannin with a modulus of elasticity of 3907MPa, then the one formulated with *KSPN* tannin with a value of 3315MPa, and finally the one with *DSSN* tannin which is 2363MPa. This result can be justified by several factors, notably the number of free reactive sites, polymer chain arrangement, the degree of polymerization, the type of interflavanoid linkages, the natural variability of tannins, and steric hindrance [33]. The resin formulated with (SPL) tannin has better crosslinking simply because in this tannin we have alpha-copaene, gamma-cadinene (terpenes), Tau-Cadinol, and eriodictyol molecules where there are easily accessible pi electrons, as well as several –OH functions, thus increasing the reactivity of this tannin towards the hardener. In the (*ADB*) tannin, several terpenes were identified, but these do not possess enough pi electrons, and those available are influenced by steric hindrance, which reduces its diffusion rate with the hardener. The N-methyl 4-hydroxypipecolic molecule found in the (*KSP*) tannin is responsible for the low reactivity of this resin. Indeed, the –CH3 group carried by the nitrogen atom makes its non-bonding pair unavailable. The low reactivity of the (*DSS*) tannin could be explained by the length of its molecular chains, reducing the mobility of reactive species. The results obtained from this analysis are better than those of resins formulated with hexamine and tannin from *Sumac* (2282MPa), *Pomegranate* (2100MPa), *Mimosa* (2665MPa), *Quebracho* (2464MPa), *Aleppo Pine* (2500MPa) (Saad et al., 2014). This highlights the high performance of the different resins formulated in this study.

 doi:10.20944/preprints202506.0750.v1

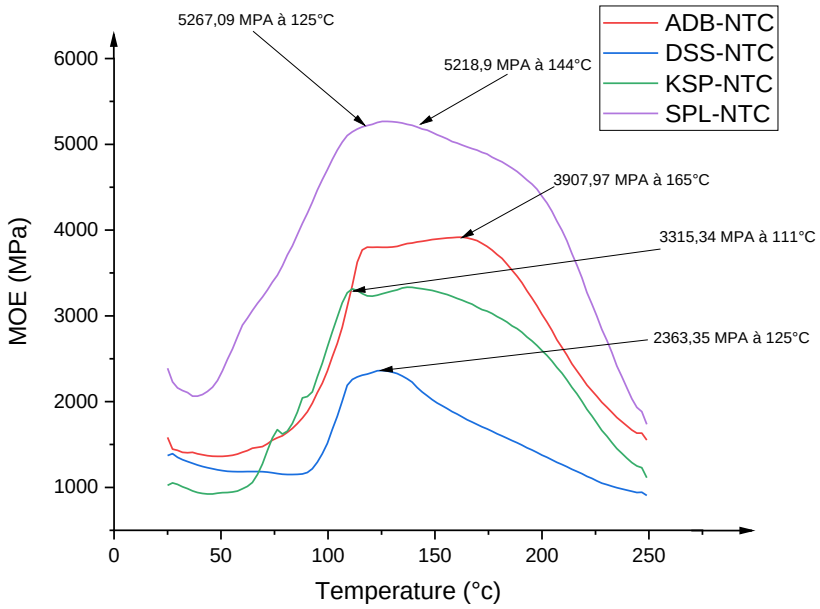

Figure 10. Superimposition of TMA spectra of the different tannins formulated with the Acacia nilotica hardener.

3.7. Comparative Study of Characterized Tannins with Those from Literature

Table 4 synthesizes the characteristics of tannins from tropical and commercial woods from recent studies, as well as those of the tannins that were the focus of this research. The observation made is that the tannins from this research possess good qualities, even surpassing those previously studied and already commercialized. Thus, the tannins from this research prove to be competitive.

Table 4. Comparative study of characterized tannins with those from literature.

Species	Part of the tree used	Nature of tannin	Extraction yield (%)	Extraction method	Maximum temperature (Tmax, °C)	Thermo mechanical analysis of the resin (MPa)	Gel time	Applications	References
Tannins from tropical woods									
Paraberlinia bifoliolata	Bark	Condensed	35%	Hot Extraction in Aqueous Solution	-	4840	-	Adhesives for panels and corrosion inhibitors	(Nga et al., 2024)
Daniellia oliveri	Bark	Condensed (flavonoids, catechins)	29%	Hot Extraction in Aqueous Solution	-	2370	790 s	Adhesives for Fiberboard	(Konai et al., 2021)
Aningre (Aningeria spp)	Bark	Condensed	19%	Hot Extraction in Aqueous Solution	-	1191	-	Resins for particleboard	(Konai et al., 2015)

 doi:10.20944/preprints202506.0750.v1

Piptadeniastrum africanum	Bark	Condensed	-	Hot Extraction in Aqueous Solution	-	3909	660 s	Adhesives for Fiberboard	(Wedaïna et al., 2021)
Ficus sycomorus	Barks	Condensed	46%,	Hot Extraction in Aqueous Solution	-	7050	600 s	Adhesives for Fiberboard	(Konai et al., 2021)
Butyrospermum parkii	Barks	Condensed	40%	Hot Extraction in Aqueous Solution	-	46210	701 s	Adhesives for Fiberboard	(Konai et al., 2021)
Azadirachta indica	Barks	Condensed	35%.	Hot Extraction in Aqueous Solution	-	2650	762 s	Adhesives for Fiberboard	(Konai et al., 2021)
Ficus platyphylla	Barks	Condensed	-	Hot Extraction in Aqueous Solution		2091	-	Adhesives for particleboard	(Ntenga et al., 2017)
Vitellaria paradoxa	Barks	Condensed	-	Hot Extraction in Aqueous Solution		1989	-	Adhesives for particleboard	(Ntenga et al., 2017)
Cissus dinklagei	Barks	Condensed		Hot Extraction in Aqueous Solution	300 °C	3825	-	Adhesives for particleboard	(Njom et al., 2024)
Aningeria altissima	Barks	Condensed	25.52 %	Hot Extraction in Aqueous Solution	325 °C	5491.77	840 -1201 s	Adhesives for Fiberboard	(Mewoli et al., 2023)
Gilbertiodendron dewevrei	Barks	Condensed	-	Hot Extraction in Aqueous Solution	-	1684.95, 6209.24, 2221.33, 7762.31, 3671.42, 1930.3	523 s, 584 s, 669 s, 744 s, 752 s, 783 s	Adhesives for Fiberboard	(Ndiwe et al., 2020)
Commercial tannins									
Pinus maritimus	Bark	Polylavonoide tannin	-	Hot Extraction in Aqueou	-	2770 3050 3250 3500	39s -585s	Adhesives for particleboard	(Navarrete et al.,

 doi:10.20944/preprints202506.0750.v1

				s Solution					2013), (Navarrete et al., 2010)
Schinopsis balansae	Commercialized	Polylavonoide tannin		Industrial	-	-	238s	Adhesives for particleboard	(Jorda et al., 2022)
Studied tannins									
Entandophragma candolei	Bark	Condensed	40 %	Hot Extraction in Aqueous Solution	340 °C	3315	448s		
Entandophragma cylindricum	Bark	Condensed	35 %	Hot Extraction in Aqueous Solution	280 and 310 °C	5267	431s		
Afzelia africana	Bark	Condensed	33 %	Hot Extraction in Aqueous Solution	200 and 250°C.	2363	430s		
Dacryodes klaineana	Bark	Condensed	25 %	Hot Extraction in Aqueous Solution	525 °C	3907	427s		

4. Conclusions

This article presents the identification and characterization of new sources of tannins from tropical woods, intended for integration into the formulation of resins for the panel industry and inhibitors. 13C NMR and MALDI-TOF analysis allowed for the determination of the chemical properties of the tannins, while the characteristics of the resins were established through gel time and thermomechanical analysis. TGA was used to determine the thermal characteristics of the resins and tannins. The tannins extracted from the barks of *Entandophragma candolei*, *Entandophragma cylindricum*, *Afzelia africana*, and *Dacryodes klaineana* were all analyzed as condensed tannins whose chemical properties vary depending on each type of wood. The different formulated resins showed very long gel times, indicating the absence of aldehydes in them, highlighting their environmentally responsible nature. TGA showed that *Dacryodes klaineana* tannin has better thermal stability with a final residue of 45.05% at 600°C℃. However, the most thermally stable resin is the one formulated with *Entandophragma candolei* tannin and the *Acacia nilotica* hardener because it forms a well-developed polymer network with the *Acacia nilotica* hardener, with a final residue of 36.72%. In general, crude tannins (from *Entandophragma cylindricum, Afzelia africana*, and *Dacryodes klaineana*) perform better than their associated resins, benefiting from better heat resistance. Thermomechanical analysis shows good performance for all resins, with the resin formulated with *Entandophragma cylindricum* tannin and the *Acacia nilotica* hardener having the highest modulus of elasticity

 doi:10.20944/preprints202506.0750.v1

(5267MPa). The different tannins and resins characterized in this study are potential sources of adhesives for industry. However, for better utilization, the study will need to be optimized by using other hardeners.

Author Contributions: LN., B.N., A.B.B. and J.J.E.B., writing—review and editing, writing—original draft, methodology; J.Z.M. and M.A., methodology, data curation, supervision, formal analysis; LN., B.N., A.B.B. and J.J.E.B., writing—review and editing, validation, supervision; A.P., A.N.P. writing—review and editing, validation, supervision, conceptualization; A.P., A.P. and A.N.P., writing—review and editing, methodology, conceptualization; J.Z.M. and M.A., writing—review and editing, methodology, data curation; LN., B.N., A.B.B. and J.J.E.B, writing—review and editing, resources, project administration. All authors have read and agreed to the published version of the manuscript.

Funding Statement: no funding of statement

Data Availability Statement: The original contributions presented in this study are included in the article. Further inquiries can be directed to the corresponding authors.

Acknowledgments: This study received financial support from the Yunnan Provincial High-level.

Conflicts of Interest: The original contributions presented in this study are included in the article. Further inquiries can be directed to the corresponding author(s).

References

1. Romero, R., Gonzalez, T., Urbano, B. F., Segura, C., Pellis, A., & Vera, M. (2025). Exploring tannin structures to enhance enzymatic polymerization. *Frontiers in Chemistry*, *13*. https://doi.org/10.3389/fchem.2025.1555202
2. Mneimneh, F., Haddad, N., & Ramakrishna, S. (2024). Recycle and Reuse to Reduce Plastic Waste-A Perspective Study Comparing Petro-and Bioplastics. *Circular Economy and Sustainability*, *4*(3), 1983-2010.
3. Das, A. K., Islam, Md. N., Faruk, Md. O., Ashaduzzaman, Md., & Dungani, R. (2020). Review on tannins : Extraction processes, applications and possibilities. *South African Journal of Botany*, *135*, 58-70. https://doi.org/10.1016/j.sajb.2020.08.008
4. Pizzi, A. (2023). Little Secrets for the Successful Industrial Use of Tannin Adhesives : A Review. *Journal of Renewable Materials*, *11*(9).
5. Cano, A., Contreras, C., Chiralt, A., & González-Martínez, C. (2021). Using tannins as active compounds to develop antioxidant and antimicrobial chitosan and cellulose based films. *Carbohydrate Polymer Technologies and Applications*, *2*, 100156. https://doi.org/10.1016/j.carpta.2021.100156
6. Vera, M., Fodor, C., Garcia, Y., Pereira, E., Loos, K., & Rivas, B. L. (2020). Multienzymatic immobilization of laccases on polymeric microspheres: A strategy to expand the maximum catalytic efficiency. *Journal of Applied Polymer Science*, *137*(47), 49562.
7. Pizzi, A. (2019). Tannins: Prospectives and Actual Industrial Applications. *Biomolecules*, *9*(8), 344. https://doi.org/10.3390/biom9080344
8. Wedaïna, A. G., Pizzi, A., Nzie, W., Danwe, R., Konai, N., Amirou, S., Segovia, C., & Kueny, R. (2021). Performance of unidirectional biocomposite developed with Piptadeniastrum Africanum tannin resin and Urena Lobata fibers as reinforcement. *Journal of Renewable Materials*, *9*(3), 477-493.
9. Valenzuela, J., Leyser, E. von, Pizzi, A., Westermeyer, C., & Gorrini, B. (2012). *Industrial production of pine tannin-bonded particleboard and Medium-Density Fiberboard (MDF).*
10. Konai, N., Pizzi, A., Raidandi, D., Lagel, M., L'Hostis, C., Saidou, C., Hamido, A., Abdalla, S., Bahabri, F., & Ganash, A. (2015). Aningre (Aningeria spp.) tannin extract characterization and performance as an adhesive resin. *Industrial Crops and Products*, *77*, 225-231.
11. Konai, N., Raidandi, D., Pizzi, A., & Meva'a, L. (2017). Characterization of Ficus sycomorus tannin using Attenuated Total Reflectance Fourier Transform Mid-Infrared Spectroscopy (ATR-FT MIR), MALDI-TOF MS and 13C NMR methods. *European Journal of Wood and Wood Products*, *75*(5), 807-815. https://doi.org/10.1007/s00107-017-1177-8

 doi:10.20944/preprints202506.0750.v1

12. Ntenga, R., Pagore, F. D., Pizzi, A., Mfoumou, E., Ohandja, L. -M. A., & others. (2017). Characterization of tannin-based resins from the barks of Ficus platyphylla and of Vitellaria paradoxa: Composites' performances and applications. *Materials Sciences and Applications*, *8*(12), 899.
13. Ndiwe, B., Tibi, B., Danwe, R., Konai, N., Pizzi, A., & Amirou, S. (2020). Reactivity, characterization and mechanical performance of particleboards bonded with tannin resins and bio hardeners from African trees. *International Wood Products Journal*, *11*(2), 80-93. https://doi.org/10.1080/20426445.2020.1731070
14. Konai, N., Pizzi, A., Raidandi, D., Lagel, M. C., L'Hostis, C., Saidou, C., Hamido, A., Abdalla, S., Bahabri, F., & Ganash, A. (2015). Aningre (Aningeria spp.) tannin extract characterization and performance as an adhesive resin. *Industrial Crops and Products*, *77*, 225-231. https://doi.org/10.1016/j.indcrop.2015.08.053
15. Konai, N., Pizzi, A., Danwe, R., Lucien, M., & Lionel, K. T. (2021). Thermomechanical analysis of African tannins resins and biocomposite characterization. *Journal of Adhesion Science and Technology*, *35*(14), 1492-1499. https://doi.org/10.1080/01694243.2020.1850611
16. Mewoli, A. E., Segovia, C., Njom, A. E., Ebanda, F. B., Eyinga Biwôlé, J. J., Xinyi, C., Ateba, A., Girods, P., Pizzi, A., & Brosse, N. (2023). Characterization of tannin extracted from Aningeria altissima bark and formulation of bioresins for the manufacture of Triumfetta cordifolia needle-punched nonwovens fiberboards: Novel green composite panels for sustainability. *Industrial Crops and Products*, *206*, 117734. https://doi.org/10.1016/j.indcrop.2023.117734
17. Njom, A. E., Voufo, J., Segovia, C., Konai, N., Mewoli, A., Tapsia, L. K., Meva'a, J. R. L., & Pizzi, A. (2024). Characterization of a composite based on Cissus dinklagei tannin resin. *Heliyon*, *10*(4).
18. Nga, L., Ndiwe, B., Biwolé, A. B., Pizzi, A., Biwole, J. J. E., & Mfomo, J. Z. (2024). Matrix Assisted Laser Desorption Ionization Time of Flight (MALDI-TOF)-Mass Spectrometry and 13C-NMR-Identified New Compounds in Paraberlinia bifoliolata (Ekop-Beli) Bark Tannins. *Journal of Renewable Materials*, *12*(3).
19. Borah, N., & Karak, N. (2022). Tannic acid based bio-based epoxy thermosets: Evaluation of thermal, mechanical, and biodegradable behaviors. *Journal of Applied Polymer Science*, *139*(11), 51792. https://doi.org/10.1002/app.51792
20. De Hoyos-Martínez, P. L., Merle, J., Labidi, J., & Charrier – El Bouhtoury, F. (2019). Tannins extraction : A key point for their valorization and cleaner production. *Journal of Cleaner Production*, *206*, 1138-1155. https://doi.org/10.1016/j.jclepro.2018.09.243
21. Saad, H., Khoukh, A., Ayed, N., Charrier, B., & Bouhtoury, F. C. -E. (2014). Caractérisation des tanins de pin d'Alep tunisien pour une utilisation potentielle dans la formulation d'adhésifs pour bois. *Industrial Crops and Products*, *61*, 517-525. https://doi.org/10.1016/j.indcrop.2014.07.035
22. Mahdi, H., Palmina, K., Gurshi, A., & Covington, D. (2009). Potential of vegetable tanning materials and basic aluminum sulphate in Sudanese leather industry. *Journal of Engineering Science and Technology*, *4*(1), 20-31.
23. Tomak, E. D., & Gonultas, O. (2018). The Wood Preservative Potentials of Valonia, Chestnut, Tara and Sulphited Oak Tannins. *Journal of Wood Chemistry and Technology*, *38*(3), 183-197. https://doi.org/10.1080/02773813.2017.1418379
24. Ghahri, S., & Pizzi, A. (2018). Improving soy-based adhesives for wood particleboard by tannins addition. *Wood Science and Technology*, *52*(1), 261-279. https://doi.org/10.1007/s00226-017-0957-y
25. Yang, T., Dong, M., Cui, J., Gan, L., & Han, S. (2020). Exploring the formaldehyde reactivity of tannins with different molecular weight distributions: Bayberry tannins and larch tannins. *Holzforschung*, *74*(7), 673-682.
26. Hafiz, N. L. M., Tahir, P. M., Hua, L. S., Abidin, Z. Z., Sabaruddin, F. A., Yunus, N. M., Abdullah, U. H., & Khalil, H. A. (2020). Curing and thermal properties of co-polymerized tannin phenol–formaldehyde resin for bonding wood veneers. *Journal of Materials Research and Technology*, *9*(4), 6994-7001.
27. Nardeli, J. V., Fugivara, C. S., Taryba, M., Pinto, E. R., Montemor, M., & Benedetti, A. V. (2019). Tannin : A natural corrosion inhibitor for aluminum alloys. *Progress in Organic Coatings*, *135*, 368-381.
28. Byrne, C., Selmi, G. J., D'Alessandro, O., & Deyá, C. (2020). Study of the anticorrosive properties of "quebracho colorado" extract and its use in a primer for aluminum1050. *Progress in Organic Coatings*, *148*, 105827.
29. Bello, A., Virtanen, V., Salminen, J. -P. , & Leiviskä, T. (2020). Aminomethylation of spruce tannins and their application as coagulants for water clarification. *Separation and Purification Technology*, *242*, 116765.

 doi:10.20944/preprints202506.0750.v1

30. Wang, G., Chen, Y., Xu, G., & Pei, Y. (2019). Effective removing of methylene blue from aqueous solution by tannins immobilized on cellulose microfibers. *International journal of biological macromolecules*, *129*, 198-206.
31. Ndiwe, B., Pizzi, A., Tibi, B., Danwe, R., Konai, N., & Amirou, S. (2019). Extraits d'exsudats d'écorce d'arbres africains en tant que bio-durcisseurs d'adhésifs tanniques thermodurcissables entièrement biosourcés pour panneaux de bois. *Industrial crops and products*, *132*, 253-268.
32. Navarrete, P., Pizzi, A., Pasch, H., Rode, K., & Delmotte, L. (2010). MALDI-TOF and 13C NMR characterization of maritime pine industrial tannin extract. *Industrial Crops and Products*, *32*(2), 105-110. https://doi.org/10.1016/j.indcrop.2010.03.010
33. Saad, H., Khoukh, A., Ayed, N., Charrier, B., & Charrier-El Bouhtoury, F. (2014). Caractérisation des tanins de pin d'Alep tunisien pour une utilisation potentielle dans la formulation d'adhésifs pour bois. *Industrial Crops and Products*, *61*, 517-525.
34. Santoso, A., Hadi, Y. S., Pizzi, A., & Lagel, M. -C. (2016). Characterization of Merbau Wood Extract Used as an Adhesive in Glued Laminated Lumber. *Forest Products Journal*, *66*(5-6), 313-318. https://doi.org/10.13073/FPJ-D-15-00080
35. Meunier Quentin, Carl, M., & Jean-Louis, D. (2015). *Les Arbres Utiles du Gabon*.
36. Scalbert, A., Mila, I., Expert, D., Marmolle, F., Albrecht, A. -M. , Hurrell, R., Huneau, J. -F. , & Tomé, D. (1999). Polyphenols, metal ion complexation and biological consequences. *Plant Polyphenols 2: Chemistry, Biology, Pharmacology, Ecology*, 545-554.
37. Zhou, X., Segovia, C., Abdullah, U. H., Pizzi, A., & Du, G. (2017). A novel fiber–veneer-laminated composite based on tannin resin. *The Journal of Adhesion*, *93*(6), 461-467. https://doi.org/10.1080/00218464.2015.1084233
38. Bikoro Bi Athomo, A., Engozogho Anris, S. P., Safou Tchiama, R., Leroyer, L., Pizzi, A., & Charrier, B. (2020). Chemical analysis and thermal stability of African mahogany (Khaya ivorensis A. Chev) condensed tannins. *Holzforschung*, *74*(7), 683-701.
39. Athomo, A. B. B., Anris, S. E., Safou-Tchiama, R., Santiago-Medina, F., Cabaret, T., Pizzi, A., & Charrier, B. (2018). Chemical composition of African mahogany (K. ivorensis A. Chev) extractive and tannin structures of the bark by MALDI-TOF. *Industrial crops and products*, *113*, 167-178.
40. Amari, M., Khimeche, K., Hima, A., Chebout, R., & Mezroua, A. (2021). Synthesis of Green Adhesive with Tannin Extracted from Eucalyptus Bark for Potential Use in Wood Composites. *Journal of Renewable Materials*, *9*(3), 463-475. https://doi.org/10.32604/jrm.2021.013680
41. Engozogho Anris, S. P., Bikoro Bi Athomo, A., Safou-Tchiama, R., Leroyer, L., Vidal, M., & Charrier, B. (2021). Development of green adhesives for fiberboard manufacturing, using okoume bark tannins and hexamine – characterization by^{1} H NMR, TMA, TGA and Differential Scanning Calorimetry (DSC) analysis. *Journal of Adhesion Science and Technology*, *35*(4), 436-449. https://doi.org/10.1080/01694243.2020.1808356
42. Pantoja-Castro, M. A., & González-Rodríguez, H. (2011). Study by infrared spectroscopy and TGA of tannins and tannic acid. *Revista latinoamericana de química*, *39*(3), 107-112.
43. Amirou, S., Zhang, J., Essawy, H., Pizzi, A., Zerizer, A., Li, J., & Delmotte, L. (2015). Utilization of hydrophilic/hydrophobic hyperbranched poly (amidoamine) s as additives for melamine urea formaldehyde adhesives. *Polymer Composites*, *36*(12), 2255-2264.